Mechanisms of negative regulation of inflammasome activation

Samuel Jeffrey Carpentier

A dissertation

submitted in partial fulfillment of the

requirements for the degree of

Doctor of Philosophy

University of Washington

2016

Reading Committee:

Brad T. Cookson, Chair

Jessica A. Hamerman

Joshua J. Woodward

Program Authorized to Offer Degree:

Microbiology

University of Washington

Abstract

Mechanisms of negative regulation of inflammasome activation

Samuel Jeffrey Carpentier

Chair of the Supervisory Committee:

Professor Brad T. Cookson

Department of Microbiology

Pyroptosis is an inflammatory program of cell death that is coordinated by the assembly of macromolecular structures known as inflammasomes. Pathogenic *Yersinia* species have evolved specific mechanisms to inhibit inflammasome activation. We identified the C-terminus of *Yersinia* virulence effector YopM is required for YopM inhibition of caspase-1 recruitment to pre-inflammasomes. Additionally, we found efficient caspase-1 activation in foci and the appearance of active caspase-1 distributed throughout the cytoplasm are important aspects of the host immune response and antagonizing these processes are key for *Yersinia* pathogenesis.

While inflammation can be beneficial in response to pathogens, excess inflammation is a serious health problem associated with organ damage resulting from infections, cancers, heart attacks, and strokes. However, host regulation of inflammasome activation is poorly understood. Through collaboration with the Hamerman lab we have identified a host protein, B-cell adaptor for PI3K (BCAP), involved in the regulation of inflammasome maturation. BCAP regulates

inflammasome activation through interactions with the host inflammasome inhibitor Flightless-I. Mechanistically, BCAP delays the recruitment of caspase-1 to the forming inflammasome through its association with the caspase-1 pseudosubstrate inhibitor Flightless-1. Thus, we have identified an inhibitory pathway that regulates inflammasome activation and innate immune cell function.

TABLE OF CONTENTS

LIST OF ABBREVIATIONS

ASC	Apoptosis-associated speck-like protein containing a CARD
CARD	Caspase activation and recruitment domain
Casp1	Caspase-1
Caspase	Cysteinyl aspartate-specific proteinase
CFU	Colony-forming units
LDH	Lactate Dehydrogenase
LPS	Lipopolysaccharide
LRR	Leucine-rich repeat
LT	Lethal toxin
NLR	Nucleotide-binding domain, LRR-containing receptor
NLRC4	NLR, CARD-containing 4
NLRP3	NLR, PYD-containing 3
MOI	Multiplicity of infection
PAMP	Pathogen-associated molecular pattern
PRR	Pathogen recognition receptor
T3S	Type III secretion
TLR	Toll-like receptor
WT	Wild-type
Yop	*Yersinia* outer protein
Ypstb	*Yersinia pseudotuberculosis*

LIST OF FIGURES AND TABLES

ACKNOWLEDGEMENTS

I would like to thank my thesis advisor, Dr. Brad Cookson, for his exceptional mentorship. He has pushed me to become a better scientist and his advice has been especially helpful for my scientific career and life. I'd like to also thank our collaborator, Dr. Jessica Hamerman for her mentorship. I would like to express my gratitude to my committee members, Drs. Jessica Hamerman, Joshua Woodward, Michael Lagunoff, Nina Salama, and Andrew Hoofnagle. I would especially like to thank Drs. Joshua Woodward and Jessica Hamerman for reading this dissertation. Finally, I would like to thank my wife Katie, for her love and encouragement.

Chapter 1. Introduction

Yersinia introduction

Yersinia pestis has caused three major pandemics in recorded history: the Plague of Justinian (which spread around the Mediterranean Sea in the 6th century), the Black Death (which spread through Europe in the 14th century), and a third pandemic (which started in China during the 19th century and spread throughout the world) (1). Throughout these pandemics it is estimated that plague has killed over two hundred million people. *Y. pestis* remains endemic throughout the world, particularly in Africa, where recent epidemics have resulted in plague being categorized as a re-emerging disease. Plague is usually transmitted to humans from a natural reservoir, such as mice and ground squirrels, although human-to-human transmission is more common with pneumonic plague, a deadlier form of disease. *Y. pestis* currently causes several thousand human cases per year and climate change may increase the risk and size of plague outbreaks. Additionally, *Y. pestis* has been weaponized and has the potential to be used as an agent of bioterrorism. Although *Y. pestis* can be treated with antibiotics, recently antibiotic-resistant isolates have recently emerged (2). These threats highlight the need for further understanding of the molecular mechanisms of *Y. pestis* virulence in order to develop strategies to combat the reemergence of this pathogen.

The pathogenic species of *Yersinia* are remarkable in their ability to inhibit mammalian inflammatory immune defenses. Inflammation caused by *Yersinia* is biphasic, consisting of a quiescent noninflammatory phase followed by a strong inflammatory response (3-6). Three *Yersinia* species cause disease in humans: *Yersinia pestis, Yersinia pseudotuberculosis* (*Y. pstb)* and *Yersinia enterocolitica*. *Y. pstb* and *Y. enterocolitica* are closely related to *Y. pestis* and cause enteritis, lymphadenitis, and occasionally systemic infection (5). *Y. pestis* shares especially

strong sequence homology with *Y. pstb* and genomic analysis indicates that *Y. pestis* evolved from *Yersinia pseudotuberculosis* between 1,500-20,000 years ago (7). Several virulence factors are remarkably conserved between the two species, therefore *Y. pstb* provides an excellent model to understand pathogenic mechanisms used by *Y. pestis*.

All pathogenic *Yersinia* share a 70kb virulence plasmid that encodes a type III secretion apparatus and secreted effectors that are termed "Yops" (8). These effectors are translocated into host cells and have been shown to aid in the evasion of innate immune responses (9, 10). While *Y. pstb* is an enteric pathogen that causes enteritis and mesenteric adenitis in humans that is generally self-limiting, *Y. pestis* is intensely more virulent in humans and is able to colonize fleas, which enables *Y. pestis* to transmit efficiently between host species. It is especially striking how a small number of genetic changes, including gene reduction resulting in inactivation of *Y. pstb* virulence factors, have led to increased virulence of *Y. pestis*.

Pathogen recognition

During microbial infections, host intracellular pattern recognition receptors (PRRs) identify pathogen-associated molecular patterns (PAMPs) to induce inflammatory immune responses (11, 12). PRRs such as nucleotide-binding domain, leucine-rich repeat containing proteins (NLRs) or Aim2-like receptors (ALRs) initiate the assembly of the inflammasome, a multiprotein complex that concentrates and activates the cysteine protease caspase-1 (11). NLRs and ALRs have similar structural organization that consist of multiple domains that contain separate functions, which include autoinhibition prior to signal recognition, homo-oligomerization after signal detection, and hetero-oligomerization with adaptor proteins or caspase-1. Active caspase-1 processes pro-IL-1β and pro-IL-18 into their bioactive forms and directs the inflammatory program of cell death known as pyroptosis. Pyroptosis contributes to

the clearance of pathogens through the elimination of an intracellular niche and recruitment of additional immune cells, particularly neutrophils.

Although protective in the context of infection, inappropriate or excessive inflammasome activation can also be detrimental, as is seen in sterile autoinflammatory diseases such as gout and pseudogout, and in autoinflammatory diseases caused by autosomal dominant activating mutations in inflammasome components such as cryopyrin-associated periodic syndromes (CAPS) with mutations in the *NLRP3* gene and Familial Mediterranean Fever with mutations in *MEFV* encoding Pyrin (13, 14). Therefore, appropriate regulation of inflammasome activation is also critical for the host.

Inflammasome assembly

Recent structural studies have revealed a nucleation dependent polymerization mechanism of inflammasome assembly, similar to the mechanism of prion polymerization (15-17). NLRs such as NLRP3 exist in an autoinhibited resting state. Upon pathogen detection NLRP3 undergoes a conformational change that overcomes autoinhibition. Intermolecular interactions between pyrin domains lead to clustering of NLRP3 molecules and recruitment of the adaptor protein apoptosis-associated, speck-like protein containing a CARD (ASC). ASC then recruits pro-caspase-1 through intermolecular interactions between caspase activation and recruitment domains (CARDs). Upon recruitment to the pre-inflammasome focus containing NLRP3 and ASC, pro-caspase-1 undergoes proximity-induced autoproteolysis to become enzymatically active. The assembly of an inflammasome focus containing NLRs, ASC and caspase-1 acts as a platform for pro-IL-1β and pro-IL-18 processing (18). Active caspase-1 also cleaves Gasdermin D, which leads to cell lysis (19, 20). Caspase-1-induced cell death, also

known as pyroptosis, is characterized by rapid pore formation in the plasma membrane, disruption of ionic gradients, and cell swelling and rupture (21). Calcium influx into pyroptotic cells induces lysosome exocytosis, which together with cell lysis result in the release of microbes, antimicrobial factors, and damage-associated molecular patterns into the extracellular space. Interestingly, recent research has shown ASC specks accumulate extracellularly and promote additional IL-1β maturation (22). These ASC specks are taken up by macrophages through phagocytosis, where they induce lysosomal damage and nucleation of soluble ASC, which leads to activation of IL-1β. Together, pyroptosis and cytokine processing result in a pro-inflammatory cascade that escalates inflammation from a local response to a systemic response.

Pathogen interference of inflammasome activation

Inflammasome activation serves to restrict a variety of pathogens, as is underscored by the numerous inflammasome inhibitors encoded by bacteria and viruses (11, 23, 24). Viruses such as KSHV (ORF63), Vaccinia virus (F1L), Measles virus (protein V), and Influenza A virus (NS1) encode proteins that target inflammasome sensors to antagonize inflammasome assembly (21, 25-27). Myxoma virus encodes the protein M013, which binds ASC and inhibits inflammasome assembly and caspase-1 activation. Orthopox virus (CrmA) and Myxoma virus (SERP2) both encode serine protease inhibitors (serpins) that inhibit caspase-1. Baculovirus and Entomopoxvirus encode p35 proteins, which also inhibit caspase-1 through a suicide substrate mechanism. Several viruses also target IL-1β, including Cowpox virus (B15R) and Vaccinia virus (B15R). The B15R proteins are IL-1R homologues that are secreted from infected cells and bind extracellular IL-1β. Additionally, Molluscum contagiosum virus (MC54L), Ectromelia virus (p13), and Yatapoxvirus (14L) all contain IL-18 binding proteins to block IL-18 signaling.

The translocated *Shigella* protein OspC3 binds the p19 subunit of caspase-4 (analogous to the p20 subunit of caspase-1) to prevent caspase-4 enzymatic activity. Inhibition of caspase-4 can extend host cell viability to give *Shigella* additional time to replicate and disseminate through the host. *Pseudomonas aeruginosa* translocates a phospholipase, ExoU, which limits caspase-1 activation through an unknown mechanism. *Coxiella burnetii* uses a type IV secretion system effector, IcaA, to prevent caspase-11 activation during co-infection with other Gram-negative bacteria. The mechanism for caspase-11 inhibition and the role of IcaA during infection are currently unknown.

Pathogenic *Yersinia* species utilize a type III secretion system to translocate *Yersinia* outer proteins (Yops) that block inflammatory signaling. All pathogenic *Yersinia* produce YopJ, YopO, YopE, YopH, and YopM. YopJ acetylates mitogen-activated protein kinases, which can lead to upregulation of non-inflammatory cell death known as apoptosis (28-31). YopO, YopE, and YopH inhibit Rho GTPases, RhoGAPs, and focal adhesion complexes, respectively (32). Some *Yersinia* species antagonize pyroptosis through the secreted effector YopK (10, 33), as YopK limits effector translocation into eukaryotic cells and likely also limits PAMP translocation and subsequent caspase-1 activation. *Yersinia pestis* also induces the host IL-1Ra, which blocks IL-1β and IL-18 signaling to suppress inflammation during infection (21). Additionally, *Yersinia* species produce competitive inhibitors of caspase-1 enzymatic activity (10, 34, 35). The bifunctional *Yersinia* type III secreted effector protein YopM binds caspase-1 as a pseudosubstrate and blocks recruitment of caspase-1 to preinflammasomes (10). YopM has been shown to inhibit the NLRC4, NLRP3, and NLRP1 inflammasomes, although it is likely that YopM inhibits additional inflammasomes, such as the AIM2 inflammasome, as the mechanism of YopM inhibition of caspase-1 is downstream of PAMP sensing. However, little is known

about the mechanism by which YopM blocks the recruitment of caspase-1 to pre-inflammasomes.

Host regulation of inflammasome activation

While many pathogen-derived proteins that interfere with inflammasome activation have been defined, relatively few host proteins that dampen this process to control potentially pathogenic inflammation have been identified. Similar to the pathogen-encoded inflammasome inhibitors, host inflammasome inhibitors either directly inhibit the proteolytic activity of caspase-1 or interfere with inflammasome assembly. Inhibitors that interfere with inflammasome assembly typically do so by expressing a single domain that can interact with NLRs or ASC, thereby blocking their ability to oligomerize and cause recruitment and activation of caspase-1. These include the pyrin-only proteins (POPs) and card-only proteins (COPs), which bind ASC or caspase-1 homotypically and do not facilitate connections to other inflammasome components (36-38). Additionally, there are host competitive inhibitors of IL-1β signaling, including IL-1Ra, and IL-1R2 (21). The host binding protein IL-18BP has a high affinity for IL-18, which reduces the circulating concentration of IL-18. Only two host proteins have been identified that directly inhibit caspase-1 through a pseudosubstrate site, the serpin PI-9 and Flightless-1 (39-41). Although Flightless-1 inhibits caspase-1 activity, little is known about the mechanisms controlling this important function.

Chapter 2. Experimental Procedures

Table 1. Bacterial strains and primers used in the YopM study

	Properties	Reference
Strains used in this study		
Ypstb	*Yersinia pseudotuberculosis* YPIII serogroup O:3. naturally deficient in YopT	(Viboud et al., 2003)
YersiniaΔ	YPIII *yopJ-, yopO-, yopE-, yopH-, yopK-, yopM-*	(Viboud et al., 2003)
ΔyopD YersiniaΔ	YPIII *yopJ-, yopO-, yopE-, yopH-, yopK-, yopM-, yopD-*	Cookson lab
ΔyopM YPIII	YPIII *yopM-*	(Viboud et al., 2003)
yopM$_{399}$ YPIII	Deletion of 10 amino acids of the C-terminus of YopM with primers 5'M$_{399}$1, 3'M$_{399}$2, 5'M$_{399}$3, and 3'M$_{399}$4	This study
Plasmids		
pBAD	pBAD30-HA	(LaRock and Cookson, 2012)
pYopM	Bacterial expression of YopM in pBAD;	(LaRock and Cookson, 2012)
pYopM$_{271A}$	Mutation of the YopM pseudosubstrate site	(LaRock and Cookson, 2012)
pYopM$_{399}$	Deletion of 10 amino acids at the C-terminus of YopM with primers 5'pM and 3'pM$_{399}$	This study
pYopM-Cya	YopM::cyaA fusion	Cookson Lab
pYopM$_{399}$-Cya	YopM$_{399}$::cyaA fusion with primers 5'pM and 3'pM$_{399}$	This study
pET	pET30 Xa/LIC	Novagen
pET-6xHis-YopM	Protein expression of YopM	(LaRock and Cookson, 2012)
pET-6xHis-YopM$_{271A}$	Protein expression of YopM$_{271A}$	(LaRock and Cookson, 2012)
pET-6xHis-YopM$_{399}$	Protein expression of YopM$_{399}$; primers 5'XaM & 3'XaM$_{399}$	This study
Primers		
ttttggatccGGAAAAATTGCCAGAGTTGC	5'M$_{399}$1	This study
ttttttctagaCTAAGTCTCATGAGCAAATTCAT	3'M$_{399}$2	This study
ttttttctagagATTTGAAACATTGCGACGA	5'M$_{399}$3	This study
ttttggatccTGCTGGTATGAAAGTTGAGCA	3'M$_{399}$4	This study
ttttGAGCTCgaaggagatatacatATGTTCATAAATC CAAGAAATG	5'pM	(LaRock and Cookson, 2012)
ttttctagaAGTCTCATGAGCAAATTCATA	3'pM$_{399}$	This study
ggtattgagggtogcATGTTCATAAATCCAAGAAATG	5'XaM	(LaRock and Cookson, 2012)
AGAGGAGAGTTAGAGCCctaagtctcatgagcaaa	3'XaM$_{399}$	This study

Table 2. Bacterial strains and primers used in the BCAP study

	Properties	**Reference**
Strains used in this study		
Salmonella	SL1344	Cookson lab
*Yersinia*Δ	YPIII *yopJ-, yopO-, yopE-, yopH-, yopK-, yopM-*	(Viboud et al., 2003)
Δ*yopM YPIII*	YPIII *yopM-*	(Viboud et al., 2003)

YopM materials and methods

Sequence alignment

YopM amino acid sequences were obtained from GenBank and aligned using MacVector.

Bacteria, plasmids and cell culture

Bacterial strains, plasmids, and primers are described in Table S1. Bone marrow-derived macrophages were differentiated from cells isolated from femur exudates of C57BL/6 (Jackson Laboratories) mice, as previously described (10). Macrophages were primed with 100 ng/ml LPS (List Biologicals) 18 hr prior to infection.

Infection conditions

For macrophage infections, *Yersinia* were grown overnight at 25°C, diluted 1:40 into LB supplemented with 20mM $MgCl_2$ and 20mM $Na_2C_2O_4$, and grown at 25°C for 1 hr, then at 37°C for 2 hrs. Bacteria containing expression plasmids were grown in media supplemented with 0.02% arabinose and 50 μg/ml carbenicillin. Bacteria were washed in PBS, added to a multiplicity-of-infection (MOI) of 10, and spun onto macrophages at 150 g for 3 min. 2 hrs post-infection, cell death was quantified by release of lactate dehydrogenase (LDH) determined by Cytotox 96 kit (Promega), following the manufacturer's protocol. In all other experiments, infections were done in media supplemented with 5 mM glycine to protect against cell lysis (42).

Immunofluorescence microscopy

Active caspase-1, both in foci and diffuse, was visualized using Fam-YVAD-FMK (Immunochemistry Technologies). Cells were washed with PBS, then fixed with Cytofix (BD).

Immunofluorescent staining of proteins was performed post-fixation in Cytoperm (BD) with antibodies specific to ASC (ADI-905-173-100, Enzo), or Caspase-1 (sc-514, Santa Cruz) with Alexa fluor-conjugated secondary antibodies (Invitrogen). Coverslips were mounted with ProLong (Molecular Probes) and examined by confocal microscope (Leica SL, Zeiss LSM 510, or Leica SP8X) at the University of Washington Wm. Keck Center for Advanced Studies in Neural Signaling. Diffuse, active caspase-1 and active caspase-1 foci were enumerated by counting the fraction of positive cells in at least eight separate fields containing 50 or more cells. Pearson's colocalization coefficients were derived using the software FIJI. All Pearson's coefficients were calculated from three independent experiments with ten cells per experiment. Where indicated, macrophages were pretreated with 10μM BI-D1870 (BML-EI407-0005; Enzo) for 3 hrs to inhibit Rsk1 kinase activity.

Immunoblotting and cytokine analysis

Supernatants from infected macrophage were sterilized by 0.22-μm filter and IL-1β release was quantified by ELISA (R&D Systems). Caspase-1 immunoblots were performed with antibody against caspase-1 p10 (sc-514, Santa Cruz), from cells lysed in pull-down lysis buffer (Thermo). Rsk-1 immunoblots were performed with antibody against Rsk1 (sc-231 AF647, Santa Cruz). GSK3β immunoblots were performed with phospho-GSK3β (Ser9) antibody (9336S, Cell Signaling Technology) and total GSK3β (9315S, Cell Signaling Technology). Actin immunoblots were performed with antibody (ab6276, Abcam Inc).

Protein interaction and functional studies

Pyroptosis was induced in 10^7 macrophages by infection with *YersiniaΔ* at MOI 10 for 2 hrs. Macrophages were then lysed with Pull-Down Lysis buffer (Thermo Fisher) and added to 10 µg of recombinant 6xHisYopM, 6xHisYopM$_{271A}$ or 6xHisYop$_{399}$ bound to HisPur Cobalt Resin (Thermo Fisher) and incubated at 4°C for 2 hrs. After four washes with binding buffer (1:1 mix lysis buffer and TBS), bound proteins were eluted with SDS-PAGE sample buffer containing 0.25 M imidazole and analyzed by immunoblot. For enzymatic assays, 10U recombinant human caspase-1 (Enzo) was pre-incubated with 6xHisYopM or 6xHisYopM$_{399}$ for 5 min at 37°C in assay buffer (Enzo) as previously described (10). Caspase-1 substrate Ac-YVAD-AMC (Enzo) was added to 200 µM and cleavage was detected by monitoring absorbance at 440 nm (Spectramax M3, Molecular Devices).

Mouse experiments

Female mice aged 6-8 wk (Jackson Laboratories) were infected by intraperitoneal delivery of 1000 CFU of *Yersinia* overnight cultures diluted in 200µl PBS after enumeration by Coulter counter (Multisizer 4, Beckman Coulter). Mice were sacrificed on day 4 and spleens were removed and placed in PBS. Spleens were then homogenized and plated for CFU. Mice were housed in specific pathogen-free conditions and experiments performed according to University of Washington Institutional Animal Care and Use Committee guidelines.

Yop secretion analysis

Following growth of *Yersinia* as described, bacteria were removed by centrifugation at 13,000 RPM for 2 minutes and trichloroacetic acid (10% w/v) was added to the supernatants to

precipitate the secreted protein. Samples were resolved on SDS-PAGE and stained with Coomassie blue.

Yop translocation analysis

Following growth of *Yersinia* as described, $2x10^5$ BMMs were infected with *Ypstb* at an MOI of 10 for 90 minutes and lysed in 0.1 M HCl. cAMP levels were measured using the Direct cAMP ELISA kit (Enzo).

Statistical analysis

GraphPad Prism was used to calculate statistical significance by unpaired Student *t* test (*P < 0.05, **P < 0.01,***P < 0.001), unless otherwise indicated. Data are representative of at least three independent experiments.

BCAP materials and methods

Mice

Wild-type C57BL/6J mice were bred at the Benaroya Research Institute or purchased from Jackson Laboratories. BCAP$^{-/-}$ mice lacking the *Pik3ap1* gene were back-crossed to C57BL/6J mice for 9 generations(43). All experiments were performed in accordance with protocols approved by the Institutional Animal Care and Use Committee at Benaroya Research Institute.

Cell Culture

Bone marrow-derived macrophages were generated from bone marrow from femurs and/or tibias of mice by culture for 7 days at 37˚C in 5% CO_2 in DMEM (Invitrogen) supplemented with 10% FCS, 5 mM HEPES, 0.2 mg/ml L-glutamine, 0.05 mM 2-ME, 50 mg/ml gentamicin sulfate, and 10,000 U/ml penicillin and streptomycin with 30% L cell-conditioned medium or 10% CMG12-14 supernatant as a source of M-CSF. Macrophages were then harvested using PBS containing 1 mM EDTA, suspended in phenol red-free antibiotic free DMEM supplemented with 5% FCS. Macrophages were activated with 100 ng/ml *Salmonella minnesota R595* LPS (List Biologicals) 18 hrs before infection or addition of inflammasome activators unless otherwise noted.

Mass spectrometry-based proteomics:

Bone marrow derived macrophages (10^8 cells/condition) were lysed with 1 ml of radioimmunoprecipitation assay buffer (RIPA; 150 mM NaCl, 50 mM Tris [pH 7.4], 1 mM EDTA (pH 8.0), 1% Triton X-100, 0.25% sodium deoxycholate, protease and phosphatase inhibitors). Immunoprecipitation was performed by incubation of lysates with 2 µg anti-BCAP antibody (4L8E6)(44) overnight (4°C) followed by subsequent enrichment using protein A

agarose beads (Calbiochem). The resulting protein complexes were washed several times in lysis buffer, twice in ammonium bicarbonate buffer (50 mM), and subsequently were reduced, alkylated and digested into peptides using Trypsin (V5280, Promega). Peptides were loaded onto a 3-cm self-packed C18 capillary pre-column (Reprosil 5 µM, Dr. Maisch). After a 10-min rinse (0.1% Formic Acid), the pre-column was connected to a 25-cm self-packed C18 (Reliasil 3 µM, Orochem) analytical capillary column (inner diameter, 50-µm; outer diameter, 360-µm) with an integrated electrospray tip (~1-µm orifice). Online peptide separation followed by mass spectrometric analyses was performed on a 2D-nanoLC system (nanoAcquity UPLC system, Waters Corp.). Peptides were eluted using a 150-min gradient with solvent A (H_2O/Formic Acid, 99.9:1 (v/v)) and B (Acetonitrile/Formic Acid, 99.9:1 (v/v)): 10 min from 0% to 10% B, 105 min from 10% to 40% B, 15 min from 40% to 80% B, and 20 minutes with 100% A. Eluted peptides were directly electrosprayed into a Orbitrap QExactive mass spectrometer (Thermo Fisher Scientific) equipped with a high energy collision cell (HCD).

The mass spectrometer was operated in a data-dependent mode to automatically switch between MS and MS/MS acquisitions. Each full scan (from *m/z* 300-1500) was acquired in the Orbitrap analyzer (resolution = 70,000), followed by MS/MS analyses on the top twenty most intense precursor ions that had charge states greater than one. The HCD MS/MS scans were acquired using the Orbitrap system (resolution = 17,500) at normalized collision energy of 28%. The precursor isolation width was set at 2 *m/z* for each MS/MS scan and the maximum ion accumulation times were as follows: MS (100ms), MS/MS (100ms). MS/MS data files were searched using the Comet algorithm(45) and the data was further processed using the Institute for System's Biology's Trans-Proteomic Pipeline(46). Static modification of cysteine (carbamidomethylation; 57.02 Da) was used in the search. For precursor area quantification of

LRRFIP2, PIK3AP1 and FLII peptides, the data files were imported into the Skyline software package(47) whereupon the retention time windows for each peptide was determined based upon co-elution the MS-MS identification. For each peptide, the relative intensity of the precursor ions was quantified using this retention time window.

Bacterial growth, in vitro infection, and inflammasome activation

Yersinia pseudotuberculosis YPIII serogroup O:3 *yopJ-, yopO-, yopE-, yopH-, yopK-, yopM-(48)* (*Ypstb*Δ) were grown overnight at 25°C in LB, then diluted 1:40 into LB with 20 mM $MgCl_2$ and 20 mM $Na_2C_2O_4$, grown at 25°C for 1 hr and then 37°C for 2 hrs. Bacteria were then washed in PBS, added to a MOI of 10, and spun onto macrophages for 3 minutes at 150g. NLRP3 was induced with 5 μM nigericin (Sigma-Aldrich). NAIP5/NLRC4 was induced with *Salmonella* grown in LB overnight at 37°C, diluted 1:40, and grown 3 hrs in LB containing 0.3 M NaCl. NAIP5/NLRC4 was induced with FlaTox, consisting of 5 μg/ml LFn-FlaA and 10 μg/ml PA (List). Recombinant LFn-FlaA was expressed and purified as previously described(49). Cytotox 96 kit (Promega) was used to determine LDH release. Experiments measuring IL-1β release, caspase-1 activation, or inflammasome assembly, were performed in the presence of 5 mM glycine to reduce cell lysis(42). To measure IL-1β release, supernatants from infected macrophages were sterilized by 0.22-mm filter and IL-1β quantified by ELISA (R&D Systems).

Immunofluorescence microscopy

Caspase-1 activation and active caspase-1 foci formation was determined by FAM-YVAD-FMK (Immunochemistry Technologies) staining of macrophages infected on glass coverslips. DNA was stained with Hoescht 33342. Cells were washed with PBS and subsequently fixed with Cytofix (BD Biosciences). Immunofluorescent staining was performed post-fixation in

PermWash (BD Biosciences) with antibodies specific to NLRP3 (sc-66846, Santa Cruz), ASC (ADI-905-173-100, Enzo), or Caspase-1 (sc-514, Santa Cruz) with Alexa fluor-conjugated secondary antibodies (Invitrogen). Coverslips were mounted with ProLong (Molecular Probes) and examined by confocal microscope (Leica SP8X) at the W. M. Keck Microscopy Center. Caspase-1 activation or foci formation was enumerated by counting the fraction of positive cells in four separate fields for each coverslip. Caspase-1 and ASC foci colocalization were enumerated by counting the fraction of positive cells in eight separate fields from duplicate coverslips.

Plasmid construction and transfection

A recombinant vector encoding murine Flightless-1 was constructed by PCR-based amplification of cDNA from mouse bone marrow derived macrophages. Truncated mutants of BCAP were generated by PCR-based mutation and amplification of wild-type BCAP expression vector(50) using Q5® Site-Directed Mutagenesis Kit (E0554S, NEB). Plasmids were transfected into 293T cells with TransIT®-LT1 transfection reagent (MIR 2300, Mirus) according to the manufacturer's instructions.

Immunoprecipitation and Immunoblot analysis

Macrophages were lysed at the indicated times in lysis buffer containing 1% Triton X-100, protease inhibitors (Sigma P8340) and sodium orthovanadate (1 mM; Sigma). For immunoprecipitation, macrophages or 293T cells were lysed using lysis buffer (50 mM Tris-HCl, pH 7.4, 150 mM NaCl, 1 mM EDTA, 1% Triton X-100, 0.25% sodium deoxycholate, 1 mM PMSF, 1 mM sodium orthovanadate and protease inhibitor (Sigma)). Whole cell lysates

were incubated with 1.5 µg anti-Flag (2 hours at 4 °C), anti-BCAP or anti-Flightless-1 antibodies (overnight at 4 °C) followed by protein A-agarose (30 minutes 4°C), extensively washed with lysis buffer, and then eluted with boiling in 1x SDS sample buffer (Invitrogen). Lysates or immunoprecipitates were separated by SDS-PAGE, transferred to polyvinylidene difluoride (PVDF) membrane, and detected by the indicated antibodies and Immobilon chemiluminescence system (Millipore). Antibodies used were to Flightless-1 (sc-55583, Santa Cruz), caspase-1 p20 (Adipogen), NLRP3 (15101S, Cell Signaling), ASC (sc-22514-R, Santa Cruz), IL-1β (AF-401-NA, R&D Systems), BCAP (4LE86)(44).

Lentivirus-Mediated shRNA Knockdown

293T cells were cotransfected with packaging plasmid (psPAX2), envelope plasmid (VSVg) together with a plasmid expressing short hairpin RNA (shRNA) specific for mouse Fli1 (TRCN0000324345, Sigma Aldrich) or non-target control shRNA (Sigma Aldrich). We transfected 293T cells in 10-cm dish and harvested the virus-containing culture medium 48 hours after changing the transfection medium to DMEM containing 10% FCS. The collected medium was filtered through 0.45-µm filters. The filtered virus were diluted in DMEM containing 10% FCS and used to infect bone marrow cells after one day of culture. 24 hours after infection, the medium was replaced with fresh macrophage medium containing 5 µg/ml puromycin. After 72 hours of puromycin selection, the macrophages were replated for further experiments.

In Vivo infection

Yersinia pseudotuberculosis YPIII *yopM- (10)* cultures were grown overnight in LB broth and enumerated by Coulter counter (Multisizer 4, Beckman Coulter). *Yersinia* were diluted in PBS

for intraperitoneal delivery of 2000 CFU in 200 µl to 6–8 wk mice. Mice were sacrificed on day 4 and spleens were homogenized and plated for CFU.

Statistical Analysis

The Student's unpaired *t* test was used in Fig. 1a-b, 2, 3, and 6b (*$p < 0.05$, **$p < 0.01$, ***$p < 0.001$), One way ANOVA with Tukey's post-test was used in Fig. 6c and the Mann-Whitney U test was used in Fig. 1d. Statistics were calculated using GraphPad Prism

Chapter 3. YopM

Here we show that the highly conserved C-terminus of YopM binds the host protein Rsk1 and is required for YopM disruption of caspase-1 spatial redistribution during infection. YopM inhibits recruitment of caspase-1 to pre-inflammasomes, which antagonizes enzymatic activation and the appearance of diffuse, active caspase-1 throughout the cytoplasm. This efficient activation and distribution of active caspase-1 is necessary for downstream processing of inflammatory cytokines and initiation of cell lysis. We further show the C-terminus of YopM is required for *Yersinia* virulence in wild-type mice and this requirement is due to a caspase-1-dependent mechanism, as the C-terminus of YopM is dispensable during *Yersinia* infection of caspase-$1^{-/-}$ mice. Together, these data indicate pathogen-induced disruption of host protein spatial regulation is an important mechanism for pathogen evasion of immune responses.

The C-terminus of YopM is required for YopM inhibition of inflammasome activation

YopM blocks pro-caspase-1 recruitment to foci (10), suggesting YopM may interact with additional proteins responsible for spatial organization of the YopM-caspase-1 complex. Because inhibiting caspase-1 is key to *Yersinia* pathogenesis, we hypothesized any such activity would be encoded by regions highly conserved in YopM. Therefore, we aligned the amino acid sequences of YopM present in numerous isolates of *Yersinia pestis, Yersinia pseudotuberculosis (Ypstb),* and *Yersinia enterocolitica* (**Fig. 1A, Supplemental Fig. 1A**). The N-terminal domain of YopM is highly conserved between sequences, likely because it encodes the signal for type III secretion (51). The caspase-1 pseudosubstrate site of YopM is also highly conserved amongst pathogenic *Yersinia* species, suggesting strong selective pressure to maintain this function (**Supplemental Fig. 1B**) (10). Interestingly, the C-terminus of YopM also displays a high level of conservation

(**Supplemental Fig. 1C**). The 23 C-terminal amino acids of YopM are disordered in the crystal structure (51, 52) and deletion of the 24 C-terminal amino acids of YopM does not considerably affect protein secondary structure, as examined by far-UV circular dichroism during urea-induced unfolding (52). Additionally, the C-terminus of YopM is required for YopM interaction with the eukaryotic kinase Rsk1 (53, 54), however the significance of this interaction is unknown. To investigate if the C-terminus of YopM is important for YopM inhibition of inflammasome activation, we created a strain of *Ypstb* expressing truncated YopM, lacking 10 C-terminal amino acids ($YopM_{399}$).

We performed a time course experiment where we infected bone marrow-derived macrophages (BMMs) with *Ypstb* strains to determine if the C-terminus of YopM contributes to YopM inhibition of caspase-1 activation. Infection of BMMs for 2 hours with *Yersinia*Δ, a *Ypstb* strain competent for type III secretion but lacking known effector proteins, results in 90% of infected macrophages with active caspase-1, while infection with *Yersinia*Δ expressing YopM results in 5% of infected macrophages with active caspase-1 (**Fig. 1B**). Mutation of the critical aspartate residue in the caspase-1 pseudosubstrate site of YopM ($YopM_{271A}$) eliminates YopM inhibition of caspase-1 activation, which results in 90% of infected macrophages with active caspase-1. Interestingly, $YopM_{399}$ has an intermediate effect on the inhibition of caspase-1 activation compared to full-length YopM or $YopM_{271A}$. 2 hours after infection of BMMs with *Yersinia*Δ expressing $YopM_{399}$ results in 35% of infected macrophages with active caspase-1, indicating $YopM_{399}$ is significantly more effective at the inhibition of caspase-1 compared to ΔYopM ($p<.001$), yet significantly inferior at caspase-1 inhibition compared to full-length YopM ($p<.001$). These results indicate the C-terminus of YopM plays a substantial role in YopM

inhibition of caspase-1 activation and suggest the C-terminus of YopM is required for efficient YopM inhibition of inflammasome activation.

Caspase-1 activation leads to rapid cell death and inflammatory cytokine processing (11, 12), therefore we quantified cell lysis and IL-1β release from BMMs during infection to determine whether the altered kinetics of caspase-1 activation resulted in a delayed inflammatory response (**Fig. 1C, D**). As previously observed, infection of BMMs with *Yersinia*Δ or *Yersinia*Δ expressing $YopM_{271A}$ led to high levels of cell lysis and IL-1β release while full-length YopM blocked cell lysis and IL-1β release. Consistent with **Fig. 1B**, infection of BMMs with *Yersinia*Δ expressing $YopM_{399}$ resulted in intermediate levels of cell lysis and IL-1β release, where $YopM_{399}$ is more effective at inhibition of cell lysis and IL-1β release compared to ΔYopM ($p<.01$, $p<.001$, respectively), yet less efficient at inhibition of cell lysis and IL-1β release compared to full-length YopM ($p<.01$, $p<.001$, respectively). Together, these findings further support a role for the C-terminus of YopM in caspase-1 inhibition.

We next examined Yop secretion and translocation with our *Yersinia*Δ expressing YopM mutants to ensure the deletion of the C-terminus of YopM does not affect YopM translocation through the type III secretion system (**Fig. 1E, F**) Indeed, we observed $YopM_{399}$ was secreted at equivalent levels compared to full-length YopM or $YopM_{271A}$ (**Fig. 1E**). Furthermore, a $YopM_{399}$-Cya fusion protein was translocated at similar levels compared to a full-length YopM-Cya fusion protein (**Fig. 1F**). These findings are consistent with previous work, which indicated a deletion of the C-terminus of YopM does not affect protein stability (52). We conclude $YopM_{399}$ is stable and efficiently produced, secreted, and translocated, indicating the delayed inflammatory response observed in **Fig. 1B, C,** and **D** is due to protein activity, rather than defects in stability and delivery. This truncated protein therefore provides an opportunity to

investigate YopM protein interactions and better understand YopM inhibition of caspase-1 activation.

$YopM_{399}$ interacts with caspase-1, but not Rsk1

Direct protein-protein interactions between YopM and caspase-1 are required for YopM inhibition of caspase-1 activation (10). We consequently decided to investigate if the C-terminus of YopM affects YopM inhibition of the enzymatic activity of caspase-1. We measured caspase-1 cleavage of a fluorescently labeled substrate in the presence of purified full-length YopM or $YopM_{399}$. Consistent with previous work (10), full-length YopM inhibits the enzymatic activity of caspase-1 (**Fig. 2A**). We observed $YopM_{399}$ also inhibits caspase-1 enzymatic activity, suggesting the C-terminus of YopM is not required for direct interactions with caspase-1. We next investigated if the C-terminus of YopM affects YopM interactions with caspase-1. Purified YopM proteins were used as bait to pull-down caspase-1 from lysate from BMMs infected with *Yersinia*Δ. We found YopM and $YopM_{399}$ both bind caspase-1, confirming the C-terminus of YopM is not required for YopM interactions with caspase-1 (**Fig. 2B**). Our data also confirms the pseudosubstrate site of YopM is required for interactions between YopM and caspase-1, as $YopM_{271A}$ did not bind caspase-1. Together, these results indicate the C-terminus of YopM is required for YopM inhibition of caspase-1 activation independent of direct interactions between YopM and caspase-1.

Because we observed the C-terminus of YopM is dispensable for YopM protein interactions with caspase-1, we investigated if the C-terminus of YopM is required for YopM interactions with other proteins that may be necessary for YopM inhibition of caspase-1 activation. Previously, the C-terminus of YopM has been described to interact with the

eukaryotic kinase Rsk1 (53, 54); therefore we examined this binding with YopM mutants. Indeed, YopM and $YopM_{271A}$ interact with Rsk1, while $YopM_{399}$ does not interact with Rsk1 (**Fig. 2B**). Although the significance of YopM/Rsk1 protein interactions is unknown, YopM interactions with Rsk1 increase Rsk1 kinase activity (55, 56). We hypothesized that YopM may increase Rsk1 kinase activity to block inflammasome activation. Therefore, we utilized the Rsk-specific small molecule kinase inhibitor BI-D1870 (57), and monitored phosphorylation of the Rsk1 kinase substrate GSK3β as a measure of Rsk1 activity. While treatment of BMMs with BI-D1870 abolishes GSK3β phosphorylation (**Fig. 2C**), inhibition of Rsk1 kinase activity did not modulate the ability of YopM to inhibit caspase-1 activation (**Fig. 2D**). Together, these results confirm that the C-terminus of YopM is required for YopM interactions with Rsk1, and strongly suggest Rsk1 kinase activity does not contribute to inhibition of caspase-1 activation during *Ypstb* infection of macrophages.

The C-terminus of YopM is necessary for YopM disruption of caspase-1 spatial regulation

The C-terminus of YopM is required for efficient YopM inhibition of caspase-1 (**Fig. 1B**), but the C-terminus of YopM is dispensable for direct inhibition of caspase-1 proteolysis (**Fig. 2A**) and the kinase activity of YopM's interacting partner Rsk1 is dispensable for caspase-1 inhibition (**Fig. 2D**). Since recruitment of pro-caspase-1 to the inflammasome is important for autoproteolysis and activation, we hypothesized that the C-terminus of YopM contributes to caspase-1 inhibition through disruption of the recruitment of pro-caspase-1 to pre-inflammasomes during infection. Visualizing the subcellular distribution of ASC and active caspase-1 one hour after *Yersinia*Δ infection, we found ASC foci formation in the presence of YopM (**Fig. 3A, top row**), consistent with previous studies (10). However, full-length YopM

blocked recruitment of caspase-1 to ASC foci, while $YopM_{271A}$ and $YopM_{399}$ did not (**Fig. 3A, middle row**). These observations suggest the C-terminus of YopM is required for YopM disruption of pro-caspase-1 recruitment to pre-inflammasomes.

During *Ypstb* infection of BMMs, $YopM_{399}$ fails to inhibit active caspase-1 focus formation (**Fig. 3A**), yet BMMs infected with *Yersinia*Δ expressing $YopM_{399}$ had strikingly less active caspase-1 diffusely distributed throughout the cytoplasm compared to BMMs infected with *Yersinia*Δ or *Yersinia*Δ expressing $YopM_{271A}$ (**Fig. 3A, Supplemental Fig. 2A**). To quantify this difference and investigate the potential significance we examined the covariance of active caspase-1 and ASC foci localization using Pearson's correlation coefficient (**Fig. 3B, Supplemental Fig. 2B**). BMMs infected with *Yersinia*Δ expressing $YopM_{399}$ show significantly higher colocalization of active caspase-1 and ASC compared to BMMs infected with *Yersinia*Δ or *Yersinia*Δ expressing $YopM_{271A}$. High colocalization between ASC and active caspase-1 indicates active caspase-1 is largely in a single focus that also contains ASC, while low colocalization between ASC and active caspase-1 indicates active caspase-1 is present throughout the cytoplasm. These results also suggest that during infection active caspase-1 focus formation precedes the release of active, diffuse caspase-1 from the inflammasome.

We thus infected BMMs with *Yersinia*Δ expressing YopM mutants and quantified active caspase-1 foci (**Fig. 3C**) and diffuse, active caspase-1 (**Fig. 3D**) at 30, 60, and 90 minutes post infection. The number of active caspase-1 foci is comparable between BMMs infected with *Yersinia*Δ, *Yersinia*Δ expressing $YopM_{271A}$, and *Yersinia*Δ expressing $YopM_{399}$, indicating both the C-terminus of YopM and the pseudosubstrate site of YopM affect YopM spatial control of caspase-1 (**Fig. 3C**). However, BMMs infected with *Yersinia*Δ expressing $YopM_{399}$ had lower levels of diffuse, active caspase-1 compared to BMMs infected with *Yersinia*Δ or *Yersinia*Δ

expressing $YopM_{271A}$ (**Fig. 3D**). Additionally, during *Yersinia*Δ infection we observed active caspase-1 foci at 30 minutes post-infection (**Fig. 3C**), a time point where we did not observe diffuse, active caspase-1 (**Fig. 3D**), indicating that active caspase-1 focus formation precedes the appearance of diffuse active caspase-1 throughout the cytoplasm. Together, these data show the C-terminus of YopM is required for YopM inhibition of caspase-1 focus formation and suggest direct YopM/caspase-1 interactions delay the release of active caspase-1 from the inflammasome focus.

The C-terminus of YopM is necessary for *in vivo* inhibition of caspase-1

Proper inflammatory responses are required for host defense to bacterial infection and YopM inhibition of caspase-1 is necessary for *Yersinia* to successfully elude host inflammatory defenses (10). The initiation of inflammasome assembly is strictly regulated and inhibiting nascent inflammasome formation may be an important strategy used by *Yersinia* to colonize the host. Because the C-terminus of YopM is required for YopM inhibition of active caspase-1 focus formation, we hypothesized the C-terminus of YopM may be required for efficient *Yersinia* colonization. Therefore, we tested this hypothesis with a rigorous *in vivo* investigation by comparing the clearance of wild-type *Ypstb*, Δ*yopM Ypstb*, and *Ypstb* expressing YopM with a 10 amino acid deletion of the C-terminus (*$yopM_{399}$ Ypstb*). Wild-type *Ypstb* successfully colonized the spleens of wild-type mice, while few Δ*yopM* or *$yopM_{399}$ Ypstb* bacteria were recovered (**Fig. 4**), consistent with previous research (54). However, wild-type *Ypstb*, Δ*yopM Ypstb* and *$yopM_{399}$ Ypstb* all colonized the spleens of *caspase 1/11*$^{-/-}$ mice to similar levels. Together, these data demonstrate the *in vivo* virulence requirement for the C-terminus of YopM results from its contribution to caspase-1 inhibition.

Discussion

Proper initiation of inflammasome activation is required for optimal host defense against bacterial and viral pathogens. Pathogenic *Yersinia* species efficiently colonize the host because they effectively subvert inflammasome activation and other immune responses during infection (5, 10, 58). These results define a region of the *Yersinia* effector YopM required for efficient inhibition of inflammatory signaling, as we show that the C-terminal domain of YopM is required for YopM disruption of caspase-1 spatial regulation during infection. These results provide mechanistic insight into the kinetics of caspase-1 activation, as we found active caspase-1 focus formation precede the appearance of active caspase-1 diffuse throughout the cytoplasm.

Recent studies have shown diverse types of intracellular signaling proteins assemble into higher-ordered structures that facilitate the amplification and transmission of cellular signals during innate immune responses (59). These supramolecular organizing centers (SMOCs) increase local concentrations of signaling components, which enhance the weak allosteric interactions required for enzymatic activation (60). SMOCs respond to a variety of ligands, including PAMPs and damage-associated molecular patterns, and function to initiate apoptosis, NF-kB activation, interferon response, pyroptosis, and pro-inflammatory cytokine secretion.

The cooperativity in the assembly of these large protein complexes leads to a rapid response to ligand stimulation and generates an all-or-nothing reaction, also known as a threshold response. We show YopM blocks active caspase-1 focus formation and prevents the appearance of diffuse, active caspase-1 to avoid the threshold response of inflammasome activation. Interference with inflammasome formation is not a strategy restricted to *Yersinia*, as other pathogens have been found to target earlier steps of inflammasome assembly. For instance,

an Enteropathogenic *Escherichia coli* secreted effector protein disrupts deubiquitination of NLRP3 to prevent NLRP3 activation (25). Myxoma and rabbit fibroma virus proteins bind ASC (26, 27) to prevent inflammasome maturation. Our work confirms the final steps of caspase-1 activation are viable targets for pathogen manipulation of inflammasome assembly.

YopM is a molecular mimic of the host inflammasome inhibitor Flightless-1, as Flightless-1 also blocks caspase-1 activation through interactions between Flightless-1's pseudosubstrate domain and caspase-1 (41). An additional mechanism of host enzymatic inhibition of caspase-1 has been identified, as the serpin PI-9 contains a pseudosubstrate site that directly inhibits caspase-1 enzymatic activity (39). Several host inhibitors also block inflammasome assembly. Pyrin-only proteins (POPs) and CARD-only proteins (COPs) interact with NLRs and ASC to block oligomerization and subsequent proximity-induced activation of caspase-1 (36-38). The variety of host mechanisms that inhibit inflammasome assembly and maturation highlight the importance of precise regulation of this important inflammatory pathway. Our insights into pathogen regulation of inflammasome inhibition may provide novel opportunities for the treatment of inflammasome-related diseases, such as cryopyrin-associated periodic syndromes. Current treatments mainly target the inflammatory cytokine response generated by active caspase-1 (61, 62). These treatments do not address immune cell lysis and release of damage-associated molecules that contribute to the pathology of inflammasome-associated diseases (63). Understanding how pathogens inhibit inflammasome assembly and maturation may assist the development of additional therapeutics that target earlier steps of inflammasome activation, thus preventing the inflammatory cytokine response in addition to cell lysis and the release of inflammatory molecules.

Pro-caspase-1 consists of a CARD domain connected to p20 and p10 subunits by linker regions (18, 64). While the CARD domain of pro-caspase-1 is required for recruitment of pro-caspase-1 to ASC foci, upon autoproteolytic processing the linker domain connecting the CARD domain to the p20 and p10 subunits is cleaved (**Fig. 5A**). Our results are consistent with this model, as we observed active caspase-1 focus formation precedes the appearance of active caspase-1 diffusely distributed throughout the cytoplasm during NLRP3 inflammasome activation (**Fig. 3C, D**). Active caspase-1 focus formation is important for efficient IL-1β/IL-18 processing (18). Although during BMM infection we found *Yersinia*Δ expressing $YopM_{399}$ induced equivalent numbers of caspase-1 foci as *Yersinia*Δ, *Yersinia*Δ expressing $YopM_{399}$ induced much less IL-1β secretion from infected macrophages. We propose a model where $YopM_{399}$ delays caspase-1 activation through interactions between caspase-1 and the pseudosubstrate site of $YopM_{399}$ (**Fig. 5C**). The competition for the caspase-1 substrate site between YopM and other molecules of pro-caspase-1 delays the activation of pro-caspase-1 and cleavage of pro-IL-1β. Additionally, here we show using the $YopM_{399}$ mutant that YopM delays the appearance of active caspase-1 in the cytoplasm, which may be important for restricting access of caspase-1 to additional substrates, such as gasdermin D (19, 20). Thus, the C-terminus of YopM is not required to delay the appearance of active caspase-1 in the cytoplasm.

This work clarifies the sequential nature of caspase-1 activation, as we show during *Yersinia* infection active caspase-1 focus formation precedes the appearance of diffuse, active caspase-1 in the cytoplasm. We found the most efficient inhibition of inflammasome activation by YopM depends on the cooperative functions of disruption of caspase-1 spatial regulation and enzymatic inhibition of caspase-1. We demonstrate the C-terminus of YopM is a critical region responsible for the proper function of YopM. The C-terminus of YopM is required for YopM

disruption of spatial regulation of caspase-1, but dispensable for YopM enzymatic inhibition of caspase-1. Together, these data highlight the dynamic and overlapping strategies used by *Yersinia* to evade host immune defenses.

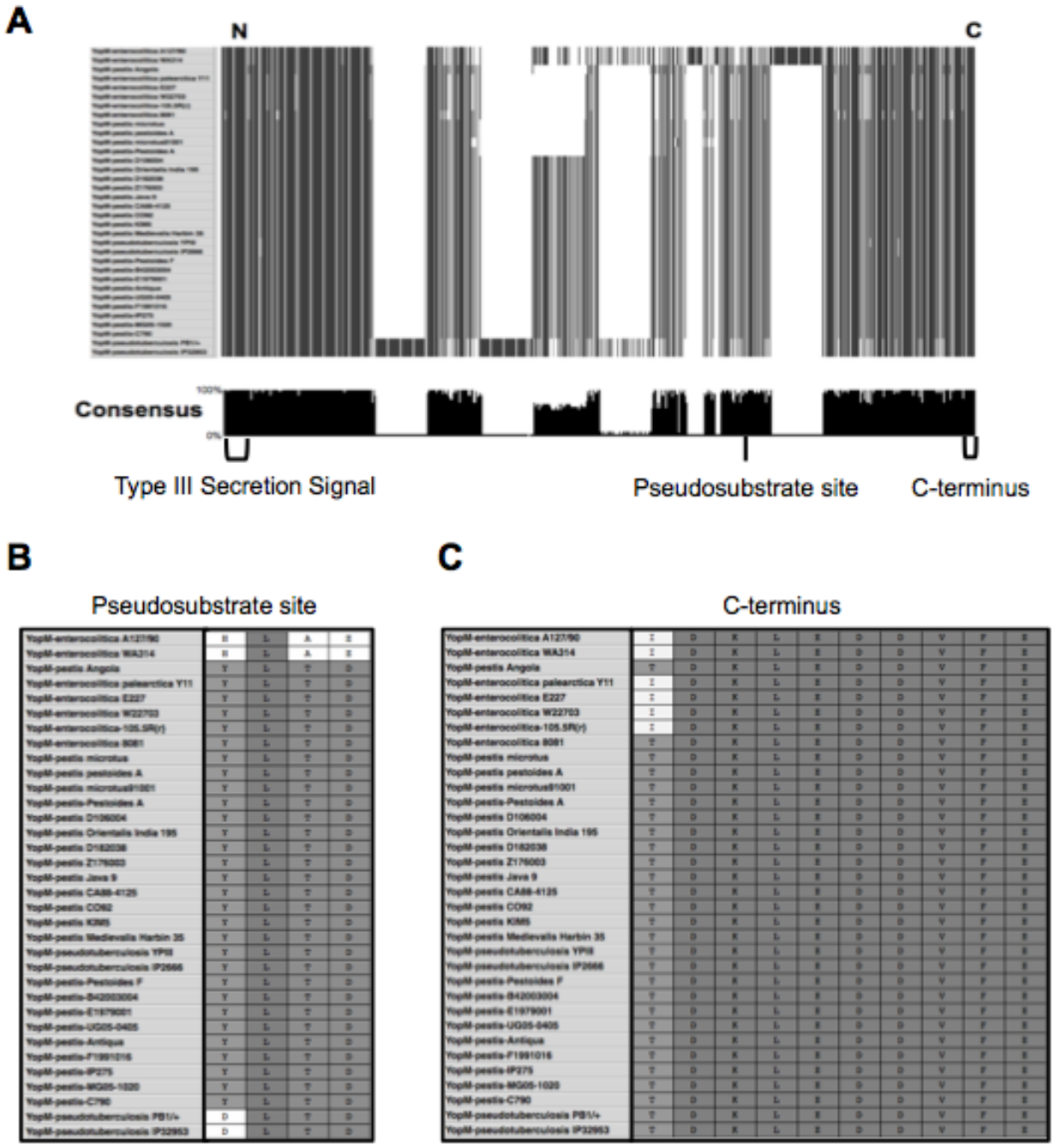

Figure 1. Supplemental Figure 1. (A) Different *Yersinia* strains encode YopM isoforms with varying numbers of leucine rich repeats. The YopM pseudosubstrate site (B) and C-terminus (C) are highly conserved amongst pathogenic *Yersinia* species.

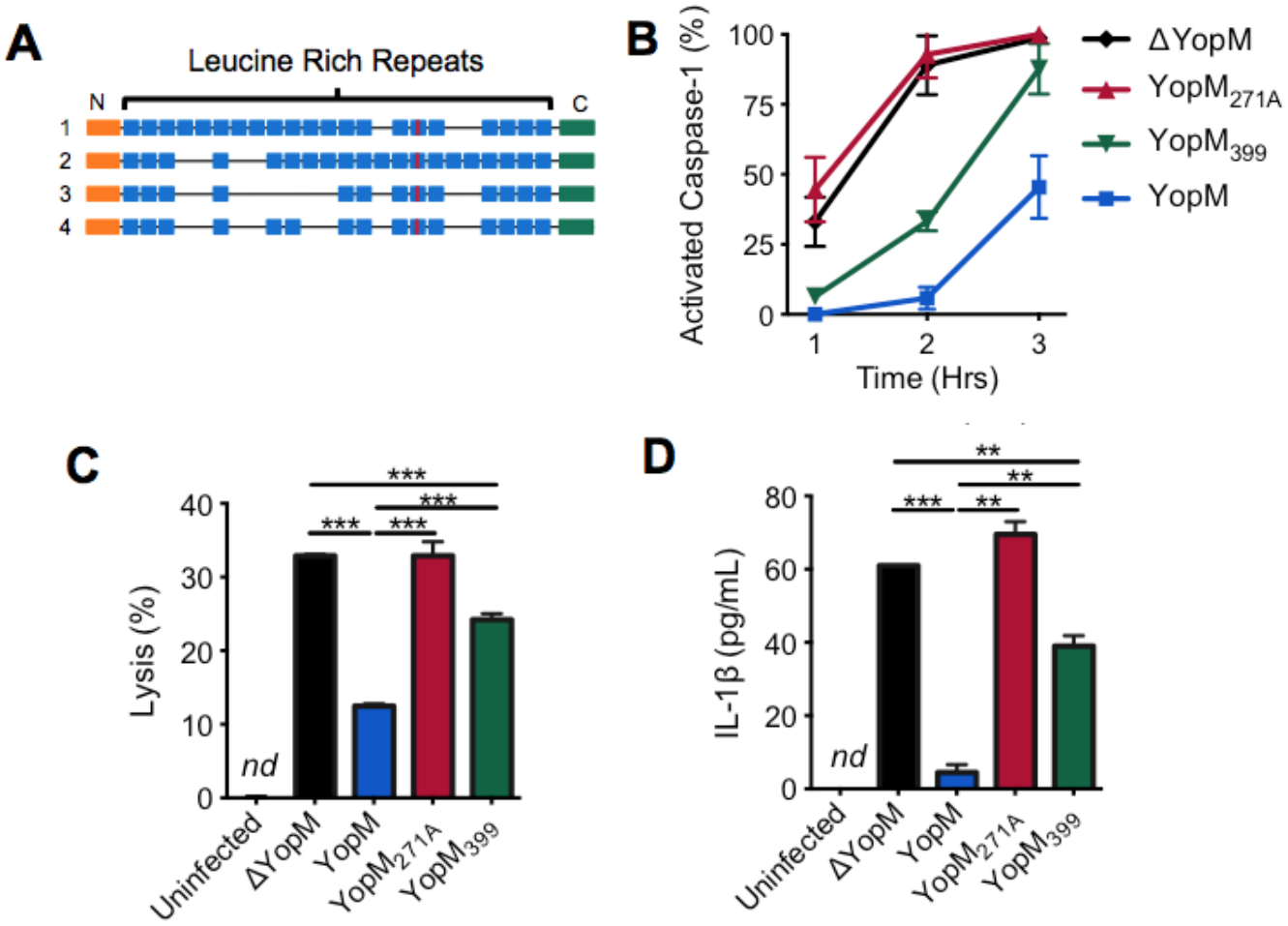

Figure 1.11 The C-terminus of YopM promotes efficient inhibition of pyroptosis during *Yersinia* infection. (A) Pathogenic *Yersinia* strains encode YopM isoforms that have varying numbers of leucine rich repeats (LRRs, blue), yet a conserved N-terminus (orange), pseudosubstrate site (red) and C-terminus (green). YopM isoforms 1, 2, 3, and 4 contain 21, 20, 13, and 15 LRRs, respectively. **(B)** The percent of macrophages with activated caspase-1 was determined during *YersiniaΔ* infection. *YersiniaΔ* expressing YopM with a deletion of 10 amino acids of the C-terminus ($YopM_{399}$) induce higher levels of caspase-1 activation compared to *YersiniaΔ* expressing full-length YopM. **(C, D)** Cellular lysis and IL-1β release were measured from macrophages infected 2 hr with *YersiniaΔ*. $YopM_{399}$ is less potent in the ability to inhibit cell lysis and IL-1β release compared to YopM. *** p<.001, ** p<.01. nd, none detectable. (**C,D** student's *t*-test). Data in (**B**) are presented as mean +/- SD, data in (**C**,**D**) are presented as mean + SD. Data are representative of three (**B,C,D**) independent experiments.

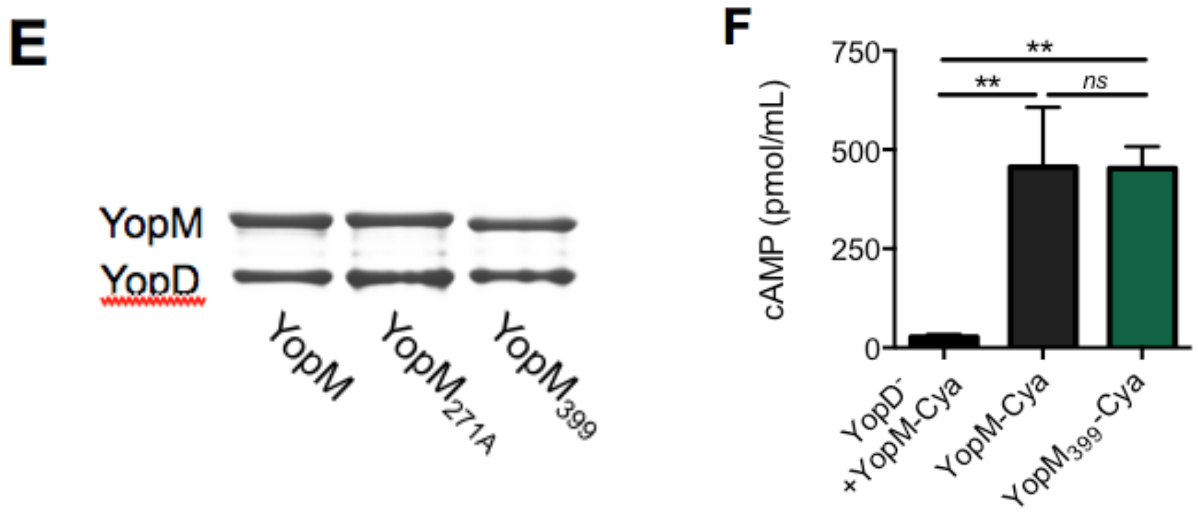

Figure 1.12. **Deletion of the C-terminus of YopM does not affect protein secretion or translocation. (E)** Secreted proteins from *YersiniaΔ* cultures were visualized through Coomassie staining. $YopM_{399}$ is secreted at equivalent levels to YopM. **(F)** Translocation of a $YopM_{399}$-adenylate cyclase fusion protein into the cytoplasm of macrophages was assessed by quantifying cAMP levels at 90 min post infection. $YopM_{399}$ is translocated at similar levels to YopM. *** p<.001, ** p<.01. ns, not significant (**C,D,E**, student's *t*-test) (**F**, One way ANOVA with Tukey's post-test). (**E**) Data are representative of three independent experiments. Data in (**F**) are presented as mean +SEM, calculated from three independent experiments.

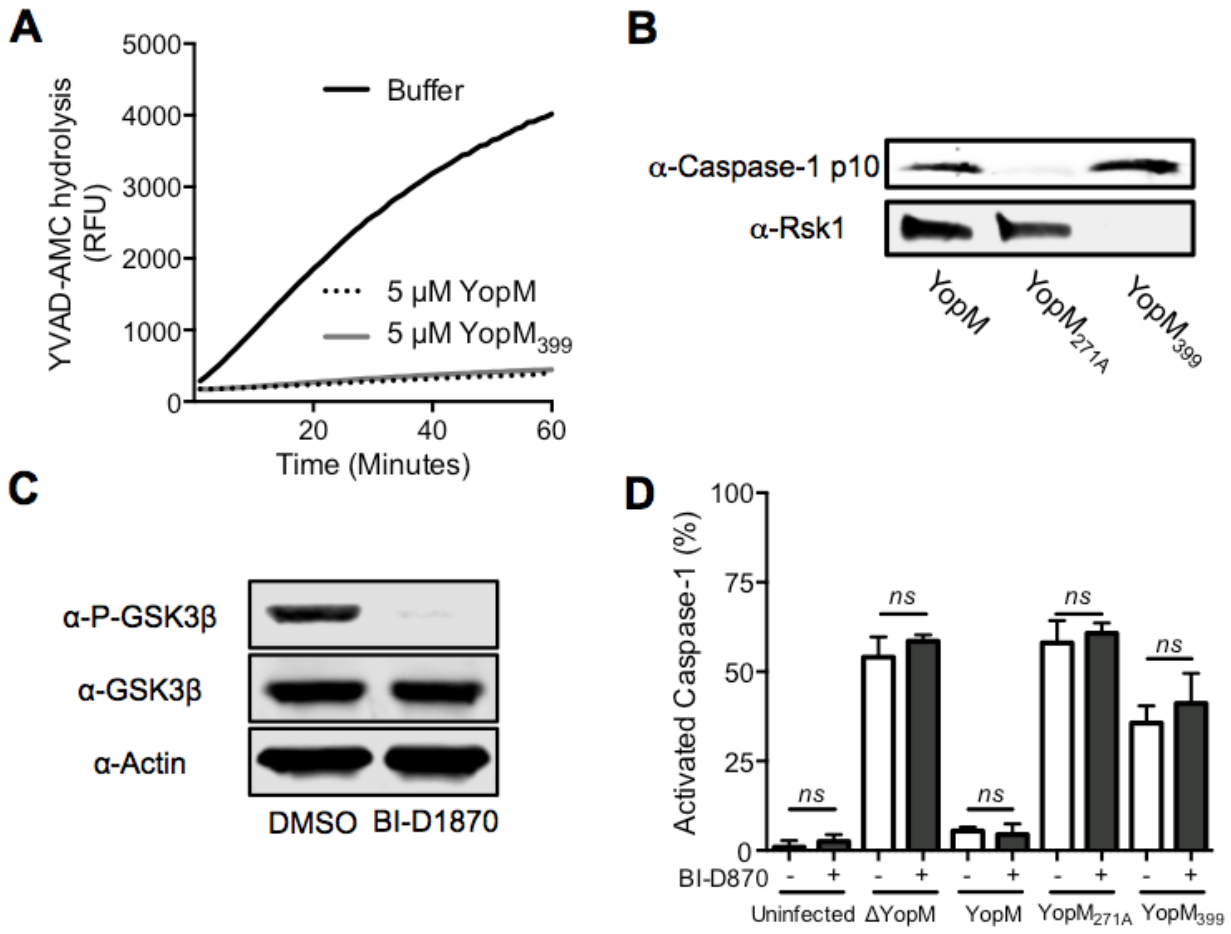

Figure 1.2. YopM$_{399}$ interacts with caspase-1, but not Rsk1. (A) Both 6xHisYopM and 6xHisYopM$_{399}$ block proteolysis of caspase-1 substrate Ac-YVAD-AMC. (B) Macrophage lysate was incubated with 6xHisYopM, 6xHisYopM$_{271A}$, or 6xHisYopM$_{399}$ as bait for pull-down and Western blot detection of Rsk1 and caspase-1. The C-terminus of YopM is required to bind Rsk1, but not caspase-1. (C) The Rsk-specific kinase inhibitor BI-D1870 inhibits phosphorylation of serine 9 of GSK3β, confirmed by Western blot. (D) Cells were pretreated for 3 hours with 10μM BI-D1870. Rsk phosphorylation does not affect caspase-1 activation during *Ypstb* infection of macrophages. ns, p> 0.05. Data in (D) presented as mean +SD.

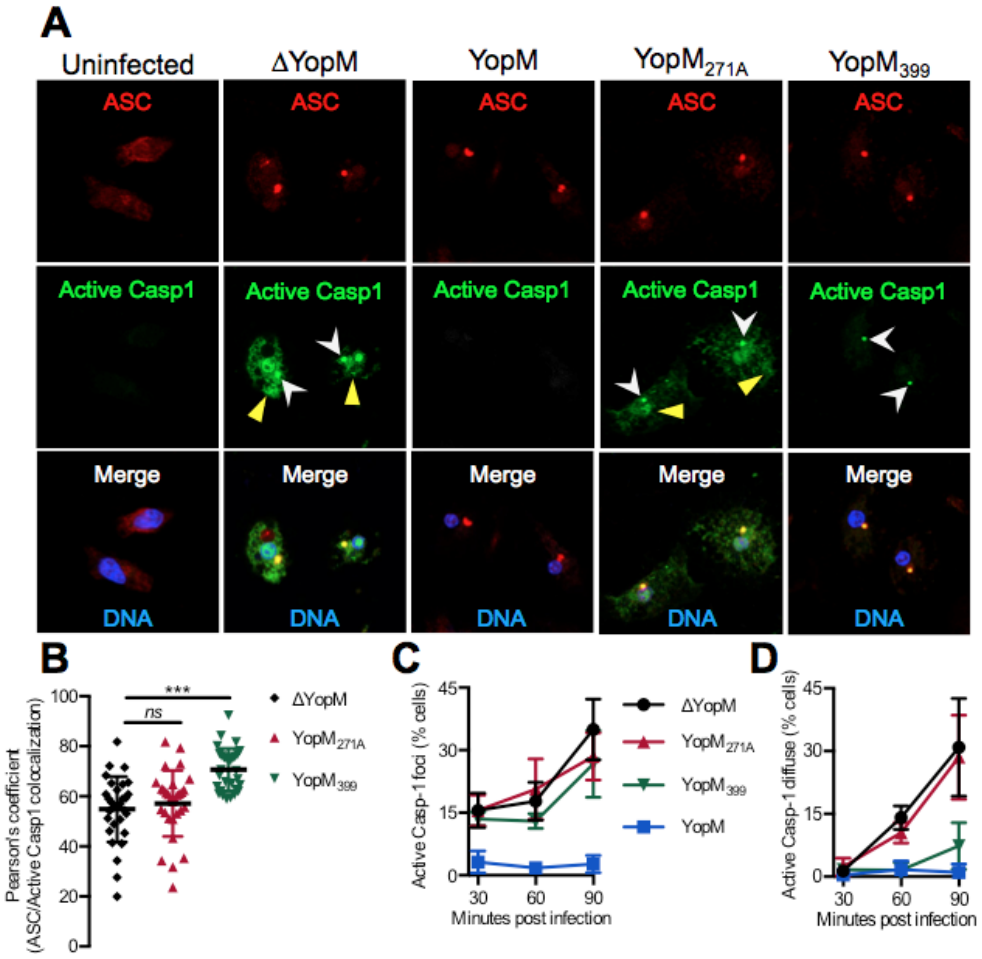

Figure 1.3. The C-terminus of YopM is required for YopM spatial regulation of caspase-1. (**A**) Macrophages were infected with *Yersinia*Δ for 2 hours and protein localization visualized by immunofluorescence microscopy. Top row: ASC (red) was stained by antibody. Middle row: Active caspase-1 (Casp1, green) was stained by FAM-YVAD-FMK. Bottom row: DNA (blue) was stained with Hoescht 33342. White arrows indicate active caspase-1 foci. Yellow arrows indicate diffuse, active caspase-1. (**B**) Pearson's correlation coefficient for ASC and active caspase-1. (**C**) Formation of active caspase-1 foci in macrophages post-infection with *Yersinia*Δ mutants. ΔYopM, $YopM_{271A}$ and $YopM_{399}$ do not block active caspase-1 foci formation, unlike full-length YopM. (**D**) Active, diffuse caspase-1 in macrophages post infection with *Yersinia*Δ mutants. $YopM_{399}$ delays the diffusion of active caspase-1 more efficiently than ΔYopM and $YopM_{271A}$. *** p<.001, ns, p> 0.05. Data in (**B,C,D**) are presented as mean +/- SD. (**B**) Pearson's colocalization coefficient was derived from three independent experiments with ten cells per experiment; each point represents a single cell.

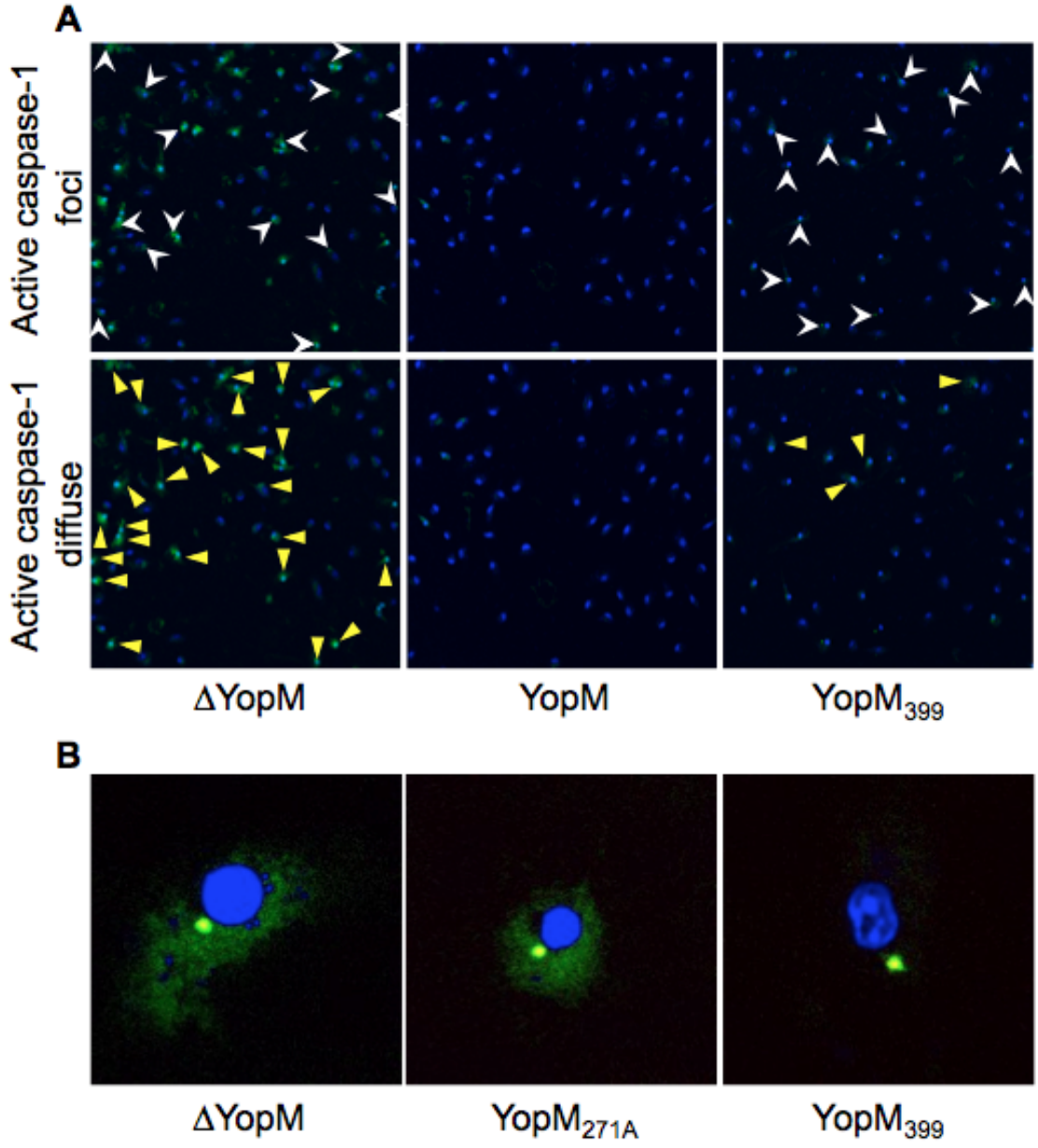

Figure 1.S.2 (A) Active caspase-1 foci formation in macrophages 2 hours post-infection with *Yersinia*Δ mutants. Active caspase-1 (green) and DNA (blue). White arrows indicate caspase-1 foci, while yellow arrows indicate diffuse, active caspase-1. $YopM_{399}$ does not block active caspase-1 foci formation, unlike full-length YopM. Additionally, $YopM_{399}$ blocks the appearance of diffuse, active caspase-1 more efficiently than ΔYopM. (**B**) Representative images from the quantification of ASC colocalization with active caspase-1. Active caspase-1 (green), ASC (red), and DNA (blue). $YopM_{399}$ blocks the appearance of diffuse, active caspase-1 more efficiently than ΔYopM or $YopM_{271A}$.

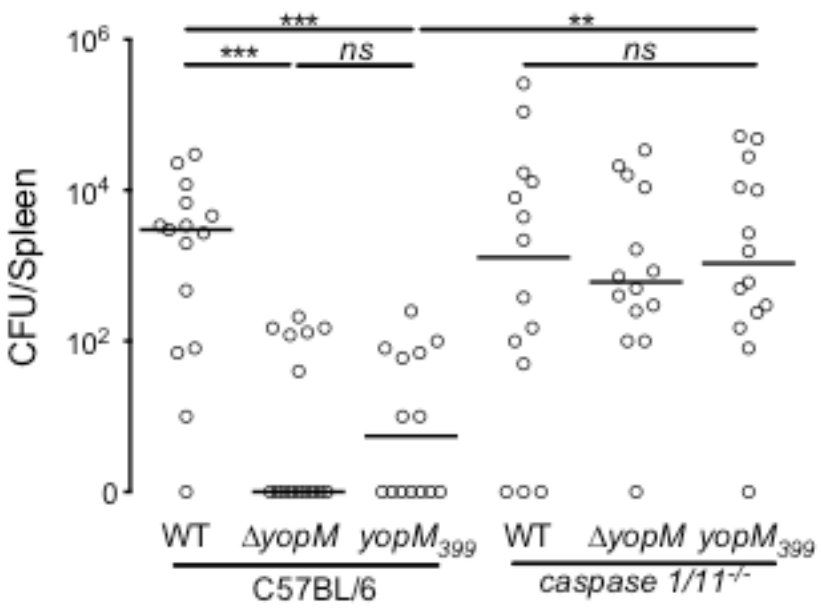

Figure 1.4. The C-terminus of YopM is required *in vivo* for inhibition of caspase-1. Splenic colonization was measured four days after intraperitoneal inoculation with 1,000 CFU *Ypstb*. Few bacteria were recovered from the spleens of C57BL/6 mice infected with Δ*yopM* or $yopM_{399}$. Δ*yopM* and $yopM_{399}$ colonize *caspase 1/11*$^{-/-}$ mice at levels similar to fully virulent *Ypstb*. Each point represents a single mouse. Results are from four combined experiments. Limit of detection was 10 CFU. Asterisks indicate statistical differences by nonparametric Mann-Whitney U test (titers, A). *** p<.001, **p<.01, ns, not significant.

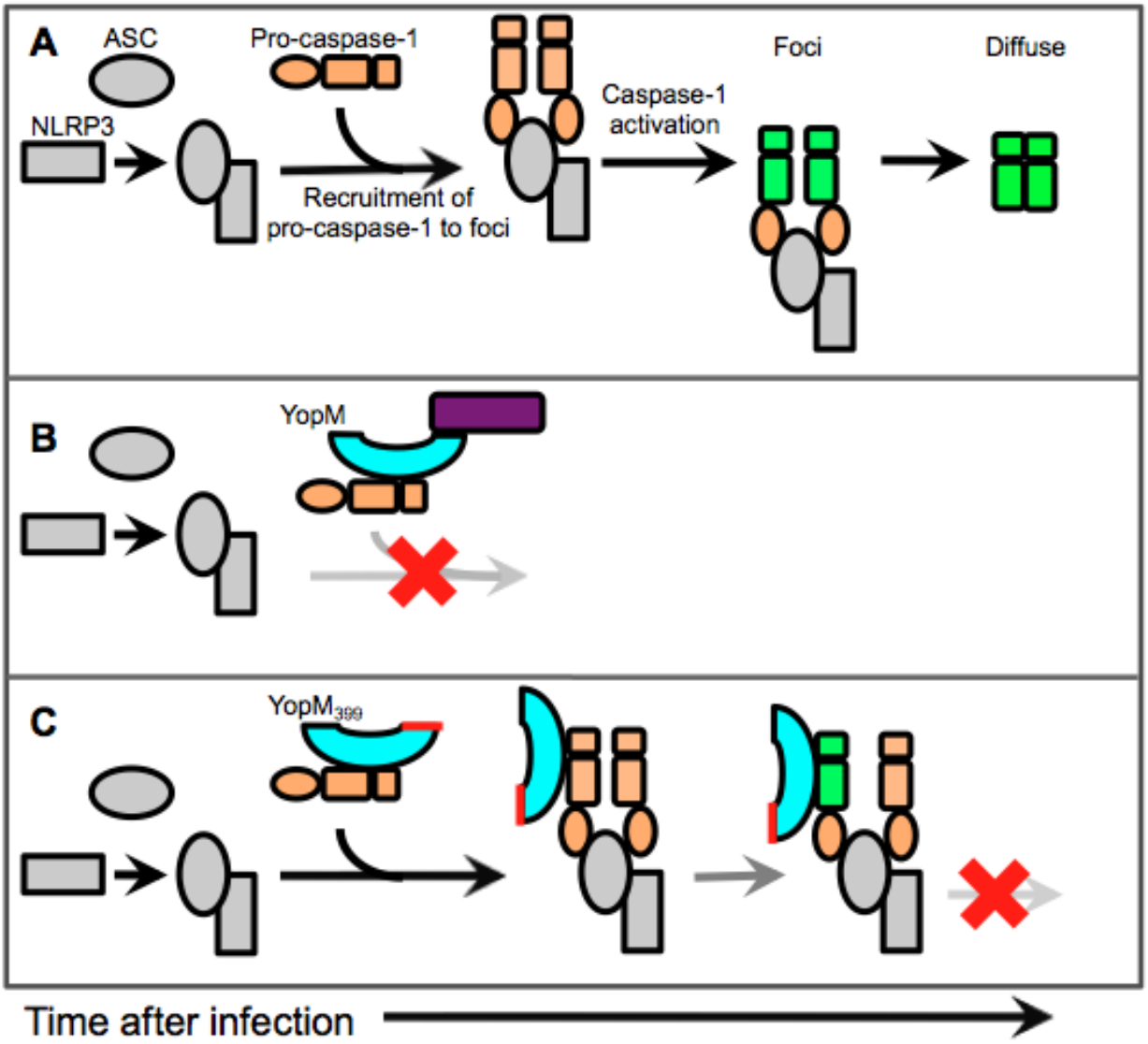

Figure 1.5. Model of YopM inhibition of inflammasome activation. (A) Pro-caspase-1 is recruited to the pre-inflammasome (NLRP3/ASC foci), where it becomes enzymatically active through proximity-induced autoproteolysis. After enzymatic activation, active caspase-1 diffuses away from inflammasome. (B) Full-length YopM interacts with pro-caspase-1 as a pseudosubstrate and blocks caspase-1 recruitment to preinflammasomes. (C) $YopM_{399}$ interacts with caspase-1 as a pseudosubstrate but is unable to block recruitment of caspase-1 to preinflammasomes. The pseudosubstrate domain of $YopM_{399}$ delays enzymatic activation and the release of active caspase-1.

Chapter 4. BCAP

Here we show the signaling protein B cell adaptor for PI3K (BCAP) blocks inflammasome activation through direct interactions with the caspase-1 inhibitor Flightless-1. During NLRP3 or NAIP5/NLRC4 inflammasome activation BCAP$^{-/-}$ macrophages activate caspase-1, undergo pyroptosis, and secrete IL-1β at an increased rate compared to WT macrophages. BCAP inhibits inflammasome activation by delaying the entry of pro-caspase-1 into the pre-inflammasome focus in a Flightless-1-dependent manner. Additionally, BCAP$^{-/-}$ mice controlled infection with a *Yersinia pseudotuberculosis* mutant whose clearance depends upon caspase-1 better than WT mice. Therefore, we have identified BCAP, as a novel mediator of Flightless-1 inhibition of inflammasome activation.

BCAP inhibits inflammasome activation

BCAP is a signaling adaptor expressed in several immune lineages, including macrophages, B cells, and NK cells. BCAP was first identified in B cells, where it becomes phosphorylated on four YxxM tyrosines after B cell receptor ligation, thereby binding and activating class I phosphoinositide 3-kinase (PI3K)(65). Work from our lab and others has shown that in macrophages BCAP links Toll-like receptor (TLR) signaling to PI3K activation, an important pathway for inhibiting TLR signaling in these cells(66, 67). BCAP is a large protein (~800 amino acids) with several protein-protein interaction domains, including 3 proline-rich sequences, a coiled-coil domain, ankyrin repeats, and a homodimerization domain(65)(68). Thus, we hypothesized that BCAP may regulate additional sensing pathways in addition to TLR. We began by investigating cytoplasmic sensing of infection by NLR leading to inflammasome activation.

We infected LPS-primed WT and BCAP$^{-/-}$ macrophages with a *Yersinia pseudotuberculosis (Ypstb)* mutant that efficiently activates the NLRP3 inflammasome. This

mutant, *Ypstb*Δ*,* has no Yop effectors to translocate into the host cytoplasm that interfere with inflammasome activation(10, 33, 48). During infection with *Ypstb*Δ*,* BCAP$^{-/-}$ macrophages had increased caspase-1 activation, cell lysis, and IL-1β secretion compared to WT macrophages (**Fig. 1a, Supplementary Fig. 1**). Thus, absence of BCAP led to increased inflammasome function in macrophages during infection with *Ypstb*Δ. To exclude that BCAP was regulating bacterial uptake or compartmentalization and thereby affecting inflammasome activation, we treated cells with nigericin, an NLRP3-activating *Streptomyces hygroscopicus* toxin(11). Again, LPS-primed BCAP$^{-/-}$ macrophages had increased caspase-1 activation, cell lysis, and IL-1β secretion compared to WT macrophages with this NLRP3 inflammasome activator (**Fig. 1b**). These data suggest that in WT macrophages, BCAP serves to inhibit inflammasome activation.

LPS priming of macrophages significantly increases NLRP3 inflammasome activation by inducing expression of NLRP3, pro-caspase-1 and pro-IL-1β. Because we have previously shown that BCAP inhibits TLR responses, we directly examined expression of components of the NLRP3 inflammasome to examine whether the increased inflammasome activation in BCAP$^{-/-}$ macrophages was due to increased LPS-priming. We found no difference between WT and BCAP$^{-/-}$ macrophages in NLRP3, ASC, pro-caspase-1 or pro-IL-1β protein by Western blot in unprimed or LPS-primed macrophages (**Fig. 1c**). We conclude that the effect of BCAP on NLRP3-induced caspase-1 activation is independent of LPS priming and therefore BCAP must regulate inflammasome activation through a post-translational mechanism.

To examine whether BCAP inhibits inflammasome activation *in vivo*, we compared the clearance of a *Ypstb* mutant solely lacking YopM, a *Ypstb* caspase-1 inhibitor, where we would expect increased inflammasome activation to result in increased bacterial clearance. *Ypstb*Δ*YopM* is attenuated compared to wild-type *Ypstb*, and this attenuation depends upon

caspase-1(10). We infected WT and BCAP$^{-/-}$ mice i.p. with ~2000 cfu *Ypstb*Δ*YopM* and measured CFU in the spleen 4 days after infection. BCAP$^{-/-}$ mice had significantly increased resistance to *Ypstb*Δ*YopM*, with ~2 logs fewer bacteria than WT mice in the spleen (**Fig. 1d**). In fact, 11/20 BCAP$^{-/-}$ mice had completely cleared the infection by day 4, whereas only 2/20 WT mice had done so. Thus, BCAP$^{-/-}$ mice have increased clearance of inflammasome-dependent bacteria compared to WT mice.

BCAP inhibits the NAIP5/NLRC4 inflammasome

We also examined inflammasome activation in unprimed macrophages after infection with *Salmonella* Typhimurium, which is principally sensed by the NAIP5/NLRC4 inflammasome and does not require LPS-priming(69). As we found with *Ypstb*Δ infection of LPS-primed macrophages, caspase-1 activation, and cell death secretion were increased in *Salmonella* Typhimurium-infected unprimed BCAP$^{-/-}$ macrophages compared to WT macrophages (**Fig. 2a)**. , IL-1β secretion was also increased in *Salmonella* Typhimurium-infected primed BCAP$^{-/-}$ macrophages compared to WT macrophages. Additionally, we observed increased cell death in unprimed BCAP$^{-/-}$ macrophages upon administration of FlaTox, a direct NAIP5/NLRC4 activator (**Fig. 2b**). FlaTox consists of *Legionella pneumophila* flagellin fused with the amino-terminal domain of *Bacillus anthracis* lethal factor, which facilitates cytosolic delivery in combination with the anthrax protective antigen channel in the absence of TLR activation(49). Together, these data strongly support a role for BCAP in suppressing caspase-1 activation downstream of NLRP3 and NAIP5/NLRC4, suggesting a general role in inhibiting inflammasome activation.

BCAP delays the entry of caspase-1 into inflammasome foci

To determine how BCAP inhibits caspase-1 activation, we examined the formation of NLRP3/ASC/caspase-1 inflammasome foci during infection with *Ypstb*Δ using immunofluorescence analysis. Upon detection of *Yersinia* infection, NLRP3 undergoes a conformational change that results in self-oligomerization into a single focus(10). This conformational change leads to NLRP3 recruitment of the adaptor protein ASC to the pre-inflammasome focus. ASC then oligomerizes and recruits pro-caspase-1, resulting in increased local concentrations of pro-caspase-1, caspase-1 focus formation and enzymatic activation(70). Because we found BCAP inhibits both the NLRP3 and the NAIP5/NLRC4 inflammasomes, we hypothesized that BCAP would not affect NLRP3 or ASC foci formation during infection, but instead would limit either the recruitment of pro-caspase-1 to the inflammasome or its subsequent proteolytic activation. Indeed, the kinetics of formation of NLRP3 and ASC foci between WT and BCAP$^{-/-}$ macrophages during infection with *Ypstb*Δ were similar (**Fig. 3a-d**), reinforcing our finding that differences between WT and BCAP$^{-/-}$ macrophages are not due to differences in NLRP3 or ASC expression after LPS-priming (**Fig. 1c**).

In contrast to NLRP3 and ASC foci formation, there was a significant increase in the recruitment of total and active caspase-1 to inflammasome foci in BCAP$^{-/-}$ macrophages compared to WT macrophages at both one and two hours after infection (**Fig. 3e-f**). Our data show that in WT macrophages there is a delay between ASC recruitment and caspase-1 recruitment to foci, unlike in BCAP$^{-/-}$ macrophages, where ASC and caspase-1 are recruited simultaneously to the inflammasome foci (**Supplemental Fig. 2**). To assess this more directly, we co-stained for ASC and active caspase-1 after *Ypstb*Δ infection. As shown in Figure 3g and h,

only ~60% of the WT macrophages with ASC foci also have active caspase-1 in the same focus at one hour after infection, while >95% of BCAP$^{-/-}$ macrophages with ASC foci have active caspase-1 in the same focus. These data show that in WT macrophages, BCAP serves to delay the entry of caspase-1 into the inflammasome focus where it becomes activated. In the absence of BCAP, entry of ASC and entry and activation of caspase-1 into the inflammasome focus are simultaneous. Thus, BCAP delays the recruitment of caspase-1 to the inflammasome, thereby dampening the proximity-induced proteolytic activation of caspase-1 and subsequent cytokine processing and cell lysis.

BCAP interacts with the endogenous caspase-1 inhibitor Flightless-1.

To identify novel BCAP-interacting proteins that may underlie the mechanism by which BCAP delays caspase-1 recruitment to the inflammasome focus, we used immunoprecipitation coupled with tandem mass spectrometry. We used a BCAP-specific monoclonal antibody in immunoprecipitation experiments from lysates isolated from WT macrophages and compared those results with BCAP immunoprecipitation from BCAP$^{-/-}$ macrophage lysates. We identified 15 proteins that met our criteria for specific BCAP interactors: at least 5 unique peptides identified in all three anti-BCAP immunoprecipitates from WT macrophages, 0 or 1 unique peptides in negative control immunoprecipitate from BCAP$^{-/-}$ macrophages, and low non-specific interactions as determined by the CRAPome database(71) (<10 average spectral counts) (**Fig. 4a**). We examined our list of specific BCAP interactors for those with defined functions in inflammasome activation, and noted the presence of two such proteins, Flightless-1 (encoded by *Flii*) and leucine-rich repeat Flightless-1-interacting protein 2 (encoded by *Lrrfip2*) (**Fig. 4a**). Interestingly, these proteins associate with each other in macrophages, where together they

inhibit NLRP3 inflammasome activation through the ability of Flightless-1 to serve as a pseudosubstrate inhibitor of caspase-1(41, 72). To quantitatively assess the presence of BCAP, Flightless-1 and Lrrfip2 in our immunoprecipitates, we performed precursor area quantification on selected peptides that we found to be abundant and to exhibit reproducible elution profiles. We quantified these peptides derived from each protein in WT and BCAP$^{-/-}$ macrophages, showing a strong enrichment in immunoprecipitates from WT macrophages (**Fig. 4b**). We then confirmed the interaction of BCAP, Flightless-1 and Lrrfip2 in macrophages by co-immunoprecipitation and Western blot (**Fig. 4c**). Together, these results demonstrate BCAP interacts with the inflammasome regulators Flightless-1 and Lrrfip2 in macrophages.

BCAP promotes the association of Flightless-1 and pro-caspase-1

We hypothesized BCAP delays inflammasome maturation through interactions with Flightless-1, therefore we examined if the association between BCAP and Flightless-1 changes after activation of the NLRP3 inflammasome. We immunoprecipitated BCAP and performed Western blotting for Flightless-1 and BCAP prior to and during nigericin-induced NLRP3 inflammasome activation. BCAP and Flightless-1 associate in LPS-primed WT macrophages prior to nigericin treatment (**Fig. 5a**), similar to what we observed in unprimed, resting macrophages (**Fig. 4c**). Strikingly, this interaction is undetectable after nigericin treatment, showing that BCAP releases Flightless-1 in response to NLRP3 inflammasome activation. We consequently investigated whether BCAP regulates the ability of Flightless-1 and pro-caspase-1 to interact. We immunoprecipitated Flightless-1 and performed Western blotting for Flightless-1 and pro-caspase-1 prior to and during nigericin treatment (**Fig. 5b**). In WT macrophages, Flightless-1 and pro-caspase-1 do not associate prior to nigericin treatment, rather this interaction

is induced during NLRP3 inflammasome activation. In BCAP$^{-/-}$ macrophages, we were not able to detect an association between Flightless-1 and pro-caspase-1 either before or during nigericin treatment. Taken together, these data indicate that following NLRP3 activation BCAP acts as a scaffold that promotes Flightless-1/pro-caspase-1 protein interaction, thereby delaying recruitment and subsequent activation of caspase-1 in the inflammasome.

We next investigated which domain of BCAP was required for its ability to bind to Flightless-1. BCAP has a variety of sequence motifs, including ankyrin repeats, a "DBB" domain shared with the drosophila protein Dof and the mammalian protein BANK1, and proline rich regions and coiled coil sequences in its C-terminal region, in addition to four tyrosines present in YxxM motifs required for p85 PI3K binding(65) (**Fig. 5c)**. To examine which BCAP region binds to Flightless-1, we constructed a panel of Flag-tagged BCAP deletion mutants and examined their ability to immunoprecipitate Flightless-1 when transfected into 293T cells. As shown in **Fig. 5d**, only the BCAP mutant lacking the N-terminal domain was unable to co-immunoprecipitate Flightless-1. Interestingly, this N-terminal domain has been reported to encode a "cryptic TIR domain" that interacts with MyD88 and TRIF in 293T transfection studies(67), suggesting this domain may be involved in BCAP regulation of TLR responses. BCAP's four YxxM tyrosines, which are required for inhibition of TLR responses(66), were not necessary for BCAP to co-immunoprecipitate Flightless-1 (data not shown). Thus BCAP uses its N-terminal domain, but does not require sequences for PI3K binding/activation, for Flightless-1 association.

Flightless-1 requires BCAP to inhibit inflammasome activation

To directly test the hypothesis that BCAP inhibits inflammasome activation through its interaction with Flightless-1, we used shRNA-mediated knockdown (KD) of Flightless-1 (Flii), which efficiently reduced Flightless-1 protein in both WT and BCAP$^{-/-}$ macrophages compared to the non-target (NT) control (**Fig. 6a**). First we examined the effect of Flightless-1 KD on the kinetics of formation of the NLRP3 inflammasome in response to *Ypstb*Δ infection in WT macrophages. As observed in BCAP$^{-/-}$ macrophages, Flightless-1 KD caused accelerated recruitment of caspase-1 to foci after *Ypstb*Δ infection, but had no effect on the kinetics of formation of NLRP3 or ASC foci (**Fig. 6b, Supplementary Fig. 3**). These data suggest that BCAP and Flightless-1 both impact inflammasome maturation at the stage of caspase-1 recruitment. To determine if BCAP requires Flightless-1 to inhibit inflammasome activation, we knocked down Flightless-1 in both WT and BCAP$^{-/-}$ macrophages and infected with *Ypstb*Δ to assess NLRP3 inflammasome activation (**Fig. 6c**). Whereas Flightless-1 KD in WT macrophages increased caspase-1 activation, Flightless-1 KD had no effect in BCAP$^{-/-}$ macrophages, proving that the interaction between BCAP and Flightless-1 is required to inhibit inflammasome activation.

Discussion

Inflammasome activation is a potent inflammatory defense required for clearance of pathogens, yet excessive inflammasome activation leads to pathological inflammation and autoinflammatory syndromes. Therefore, tight regulation of this pathway is required to resist infection, yet prevent excess collateral damage. In this study, we show that the signaling adaptor protein BCAP dampens inflammasome activation through interaction with the endogenous caspase-1 inhibitor Flightless-1. Together, BCAP and Flightless-1 delay pro-caspase-1 recruitment to pre-inflammasomes to inhibit inflammasome activation. Thus, we not only have

identified a protein complex necessary for the regulation of inflammasome formation, but also defined a novel mechanism of action for the caspase-1 pseudosubstrate inhibitor Flightless-1.

Inflammasomes are modular structures, in which multiple sensor molecules can combine with the adaptor molecule ASC to serve as a scaffold that recruits the effector molecule pro-caspase-1(61). For example, the sensor proteins NLRP1, NLRP3 and AIM2 sense a variety of distinct ligands, yet these proteins contain pyrin or CARD domains responsible for the recruitment of ASC. Similarly, the sensor NAIP proteins recruit NLRC4, which contains a CARD domain that is required for the recruitment of ASC and pro-caspase-1(11). Here, we show that BCAP inhibits both NLRP3 and NAIP5/NLRC4 inflammasomes. Because BCAP and Flightless-1 target the final step in inflammasome assembly, the recruitment and proteolytic activation of pro-caspase-1, it is likely that BCAP and Flightless-1 inhibit other inflammasomes in addition to those initiated by NLRP3 and NAIP5/NLRC4, such as the NLRP1 and AIM2 inflammasome complexes.

Our results reveal a mechanism used to modulate the spatially dependent signaling events of inflammasome formation, as BCAP and Flightless-1 work cooperatively to delay pro-caspase-1 recruitment to forming inflammasomes containing NLRP3 and ASC. Flightless-1 is a bifunctional inhibitor of inflammasome activation, as Flightless-1 not only delays pro-caspase-1 recruitment to the assembled NLRP3/ASC pre-inflammasome, as is shown in this study, but it also inhibits the enzymatic activity of caspase-1 as a pseudosubstrate(41). The bifunctional inflammasome inhibition by Flightless-1 is similar to the mechanism of inhibition of the *Yersinia* effector YopM, which also inhibits caspase-1 as a pseudosubstrate and blocks recruitment of pro-caspase-1 to NLRP3/ASC foci during infection(10). The fact that both Flightless-1 and YopM use pseudosubstrate inhibition and delay of pro-caspase-1 recruitment to the forming

inflammasome focus to disrupt inflammasome activation suggests that other identified caspase-1 pseudosubstrate inhibitors may be similarly bifunctional.

Interestingly, enzymatic studies with purified caspase-1 show that YopM is a more potent caspase-1 inhibitor than Flightless-1, highlighting the distinct roles of host-encoded and pathogen-encoded inflammasome inhibitors(10, 41). Potently blocking caspase-1 activation is an essential method of immune evasion by a pathogen, such as *Ypstb*. Conversely, host-derived inhibitors such as Flightless-1 should ensure a threshold of activation is met before initiating the all-or-none process of inflammasome activation, in order to mount a proper immune response without excessive inflammation. The existence of other host inhibitors of inflammasome assembly, such as POPs and COPs that block assembly further upstream than Flightless-1, further highlight the importance of tight control over caspase-1 activation. These mechanisms of inflammatory inhibition serve to fine-tune the inflammatory response to limit the damage associated with excess inflammation and to ensure these potent responses are limited to situations of true peril to the host.

In addition to its function as a caspase-1 pseudosubstrate inhibitor, Flightless-1 also acts as an actin capping protein through interactions of its gelsolin domain with F-actin, and thus is found in F-actin-rich regions such as podosomes and lamellopodia in fibroblasts and epithelial cells(41). Interestingly, in our mass spectrometry analysis of BCAP interacting proteins where we identified Flightless-1, we also found proteins that bind to or regulate the actin cytoskeleton, including several myosins, gelsolin, and components of the Arp2/3 complex(73, 74). This suggests interactions between BCAP and the actin cytoskeleton could be involved in BCAP inhibition of inflammasome activation. Overexpression of Flightless-1 in HeLa cells can cause the redistribution of caspase-11 to actin rich structures, but this was not examined with caspase-1

or with physiological levels of Flightless-1 expression(41). It is possible that BCAP and Flightless-1 target pro-caspase-1 to regions of F-actin to sequester pro-caspase-1 from pre-inflammasomes. The role of the actin cytoskeleton in inflammasome activation varies by NLR, with no proposed role for actin polymerization in activation of the NLRP3 inflammasome to date. One report shows NLRC4 activation is promoted by actin polymerization during infection with *Salmonella* Typhimurium(75). Additionally, the pyrin inflammasome detects perturbations in the actin cytoskeleton caused by bacterial toxins that inhibit rho GTPases(76) or by mutations that dysregulate actin polymerization(77), though the exact mechanism by which pyrin senses these changes in actin dynamics is not known. Our findings suggest that actin may impact negative regulation of inflammasome function, through BCAP and/or Flightless-1 interactions with this cytoskeleton.

Current therapeutics that target inflammasomes largely target the inflammatory cytokine response generated by caspase-1 activation, such as the IL-1 receptor antagonist anakinra or the neutralizing IL-1β antibody canakinumab (61, 62). However, inflammasome activation also leads to immune cell lysis and the release of DAMPs that play a role in the pathology of inflammasome-associated diseases(63). Colchicine is commonly used as a treatment for inflammatory disorders such as gout, however the mechanism of action is unclear and colchicine treatment has several gastrointestinal, hematologic, and neuromuscular side-effects(62). Our studies reveal a novel inhibitor of inflammasome activation that reduces both cytokine processing and cell lysis. Future therapeutics that target the inflammasome by blocking both recruitment and activation of caspase-1, rather than by targeting inflammasome-dependent cytokines, could offer novel opportunities for the treatment of inflammatory disease. Therefore,

understanding how BCAP and Flightless-1 inhibit inflammasome activation may allow for additional methods to treat diseases characterized by pathological inflammasome activation.

Our data show that BCAP and Flightless-1 are a critical hub for inflammasome regulation in macrophages. Regulation of inflammasome activation is a novel function for BCAP, which had previously only been shown to regulate the PI3K pathway in macrophages and other hematopoietic cells such as B cells and NK cells. Here we show Flightless-1 and BCAP participate in the spatial regulation of formation of the fully active inflammasome focus containing active caspase-1, similar to the function of the *Yersinia* effector YopM. Together, this work highlights the complex interplay between negative regulators of inflammasome activation that are integrated to produce the appropriate level of inflammation, key to both protective and pathogenic immune responses.

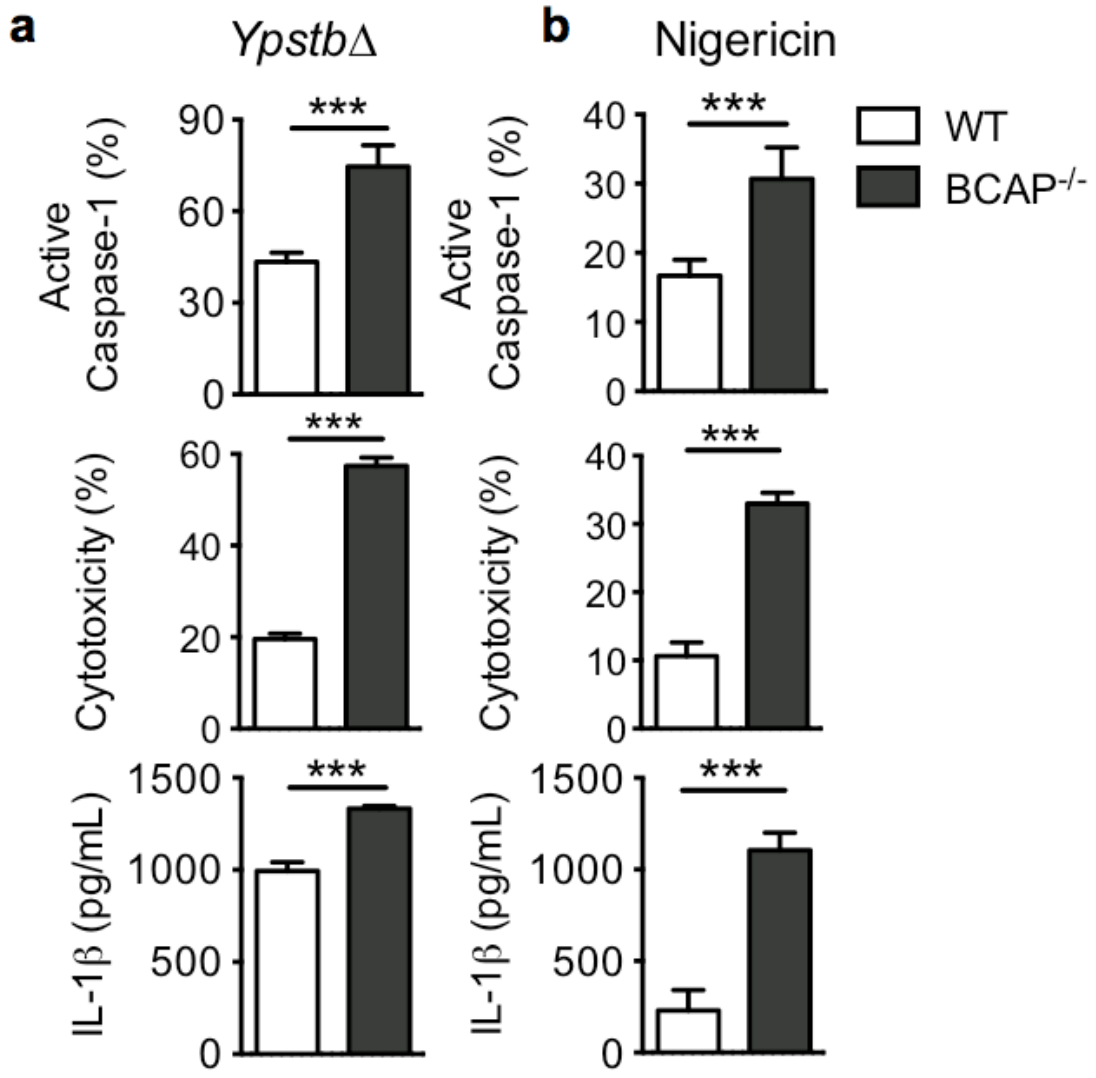

Figure 2.1.1 Increased inflammasome activation in the absence of BCAP. (a, b) WT and BCAP$^{-/-}$ bone marrow-derived macrophages (BMDM) were primed with 100 ng/ml LPS overnight after which they were infected with an MOI of 10:1 *Ypstb*Δ for 90 min (a) or treated with 5 μM nigericin for 30 min (b). (a-b) Cell death was measured by LDH release assay, IL-1β secretion by ELISA, and active caspase-1 by FAM-YVAD-FMK staining and immunofluorescent microscopy, represented as percent of cells with an active caspase-1 focus. Statistical significance was determined using a Student's *t*-test (a,b). **p*<.05, ***p* <.01, ****p*<.001. Data are presented as mean + SD (a-b).

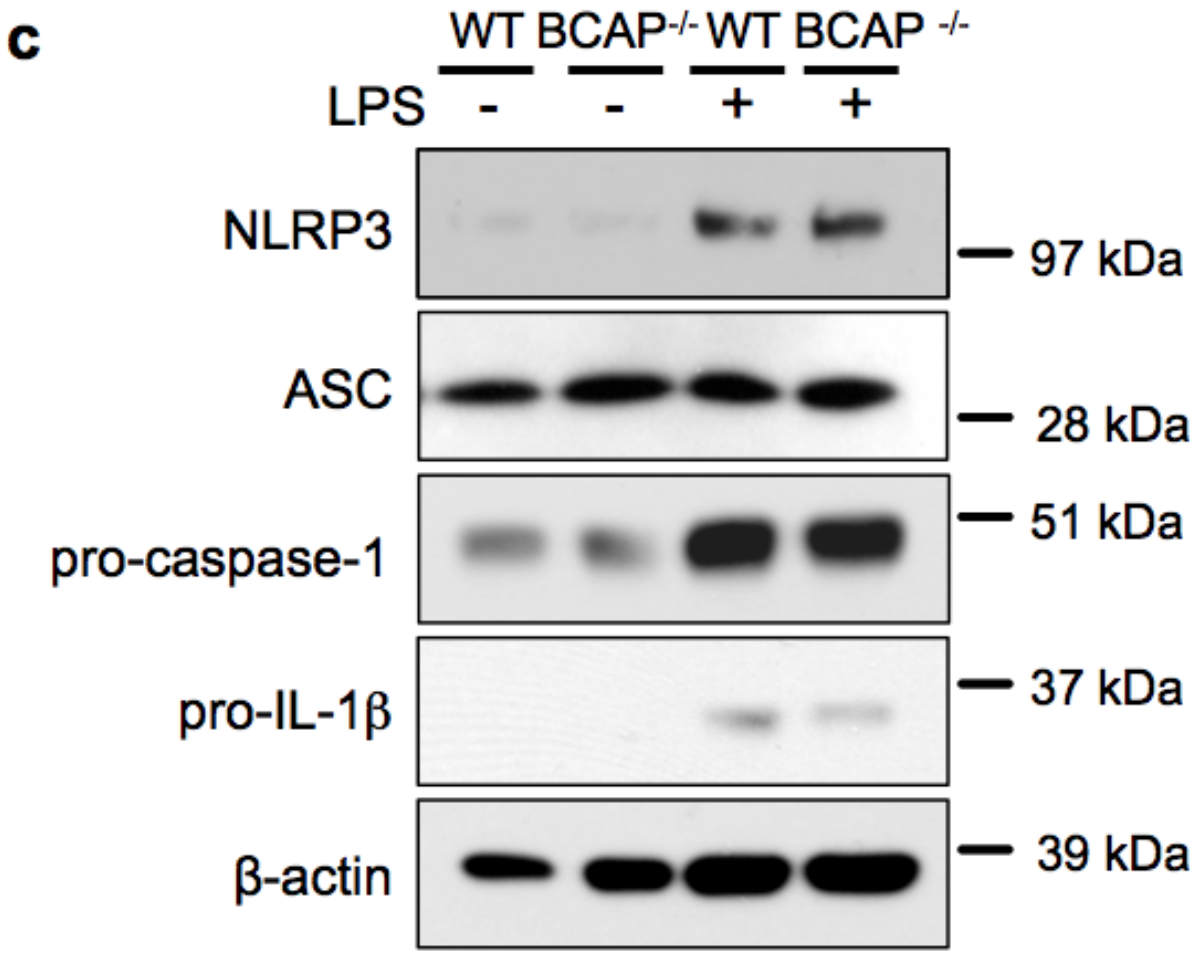

Figure 2.1.2 BCAP does not affect LPS priming of inflammasome components. (c) LPS-priming resulting in increased NLRP3, pro-caspase-1 and pro-IL-1β protein is similar in WT and BCAP$^{-/-}$ BMDM as assessed by Western blot. There was no difference in ASC protein levels between WT and BCAP$^{-/-}$ BMDM.

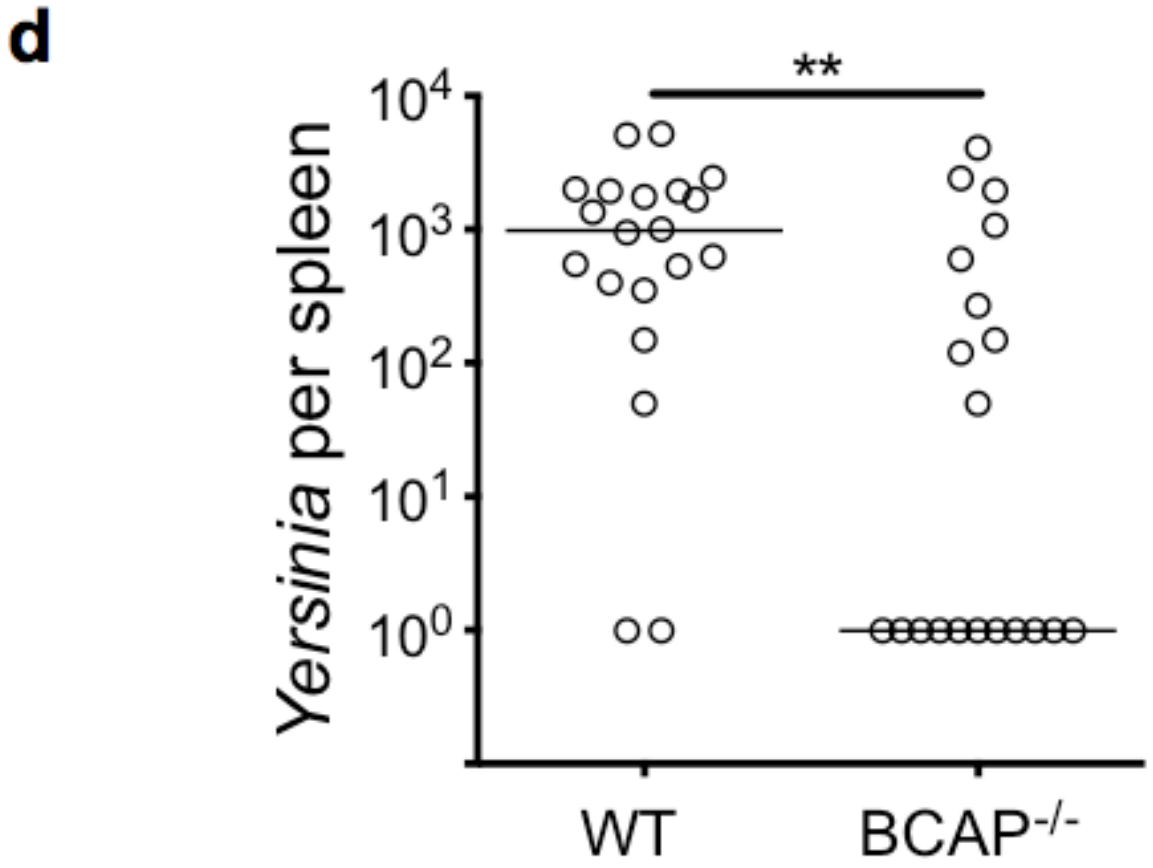

Figure 2.1.3 BCAP knockout mice are more resistant to *Yersinia* infection compared to WT mice. (d) WT and BCAP$^{-/-}$ mice were infected i.p. with ~2000 colony forming units (cfu) *YpstbΔYopM* and then cfu in the spleen were determined on day 4 post-infection. There was no difference in spleen weights between the two groups. Statistical significance was determined using a Mann-Whitney test. *p<.05, **p <.01, ***p<.001. Data are representative of three independent experiments.

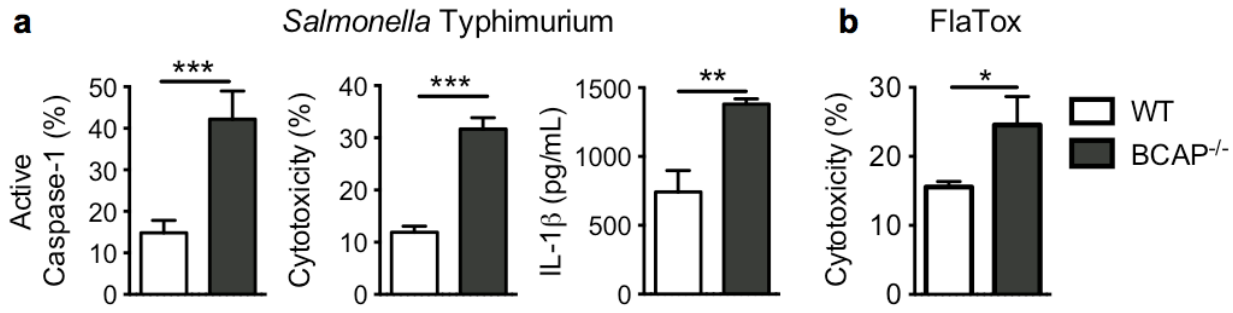

Figure 2.2. BCAP inhibits the NAIP5/NLRC4 inflammasome. (a) Unprimed (caspase-1 activation, cell lysis) and primed (IL-1β secretion) BMDM were infected with an MOI of 10:1 *Salmonella* Typhimurium for 30 minutes. For(b) Unprimed WT and BCAP$^{-/-}$ BMDM were treated with 5 μg/ml FlaTox for 20 minutes. (a-b) Cell death was measured by LDH release assay, IL-1β secretion by ELISA, and active caspase-1 by FAM-YVAD-FMK staining and immunofluorescent microscopy, represented as percent of cells with an active caspase-1 focus. **p*<.05, ***p* <.01, ****p*<.001 (Student's *t*-test). Data are representative of three independent experiments. Data are presented as mean + SD (a-b).

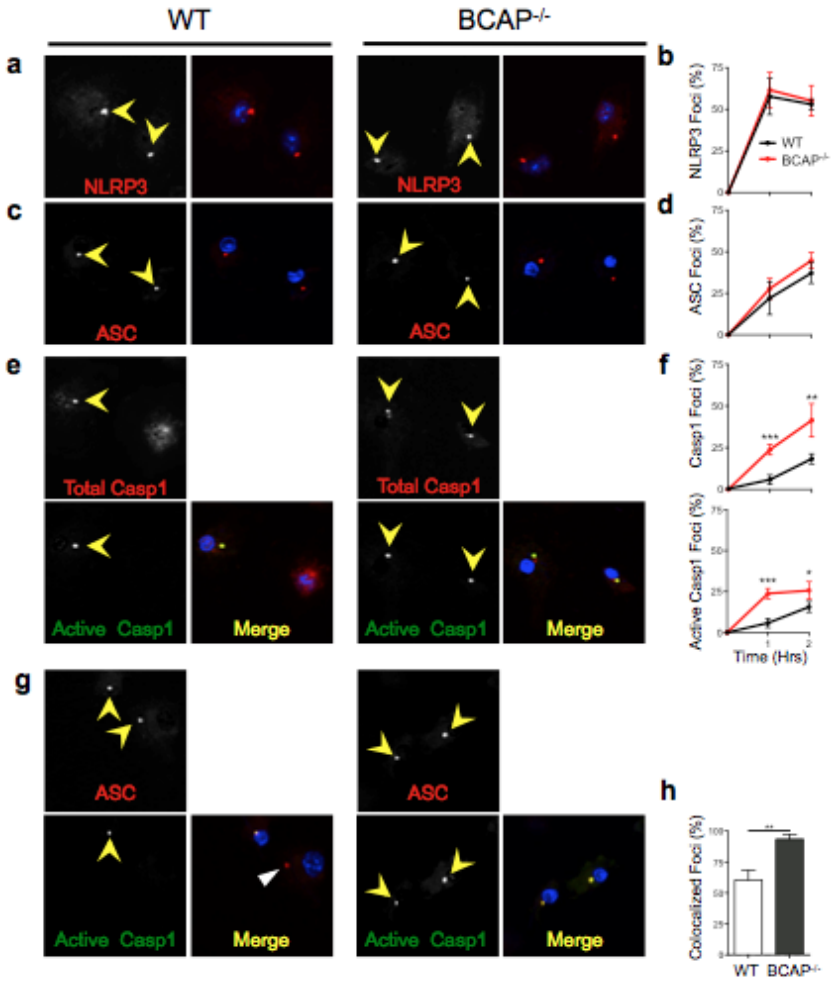

Figure 2.3. BCAP inhibits caspase-1 recruitment into the forming inflammasome focus. *(*a,c,e,g*)* BMDM were LPS-primed overnight and then infected with a 10:1 MOI *YpstbΔ* for 0, 1, or 2 hours. Cells were fixed and stained with antibodies to NLRP3, ASC or Caspase-1 and Hoescht 33342 (DNA) or stained with the fluorescent active caspase-1 probe FAM-YVAD-FMK before fixation. Yellow arrows indicate foci. Immunofluorescent images shown were taken 1 hour post-infection. (b,d,f) The percent of cells with foci of the indicated protein was quantified from four fields of at least 40 cells each. (g) One hour post-infection, cells were stained with FAM-YVAD-FMK, fixed and then stained for ASC. White arrow indicates pre-inflammasome focus containing ASC, but not active caspase-1. (h) The percent of cells with ASC foci that had co-localized active caspase-1 in the foci was quantified one hour post-infection. *p<.05, **p <.01, ***p<.001 (Student's t-test). Data are representative of three independent experiments. Data are presented as mean +/- SD (b,d,f) or mean + SD (h).

a

		BCAP IP			
		WT		BCAP$^{-/-}$	
Gene	Protein	Unique	Total	Unique	Total
MYO5A	Myosin VA	39	79	0	0
PIK3AP1	BCAP	21	68	1	3
MYO1E	Myosin IE	17	32	0	0
FLII	Flightless-1	16	30	0	0
TPM4	Tropomysin alpha4 chain	14	33	0	0
GSN	Gelsolin	13	22	0	0
TPM1	Tropomysin alpha1 chain	13	33	0	0
TMOD3	Tropomodulin13	12	30	0	0
FBN1	Fibrillin-1	12	16	0	0
LRRFIP2	Lrrfip2	11	24	0	0
ACTR3	ARP3	11	22	0	0
CAPZB	CapZ subunit beta	10	27	0	0
ARPC2	Arp2/3 complex subunit 2	9	16	0	0
CAPZA2	CapZ subunit alpha 2	8	14	0	0
LCP1	Plastin 2	8	13	0	0

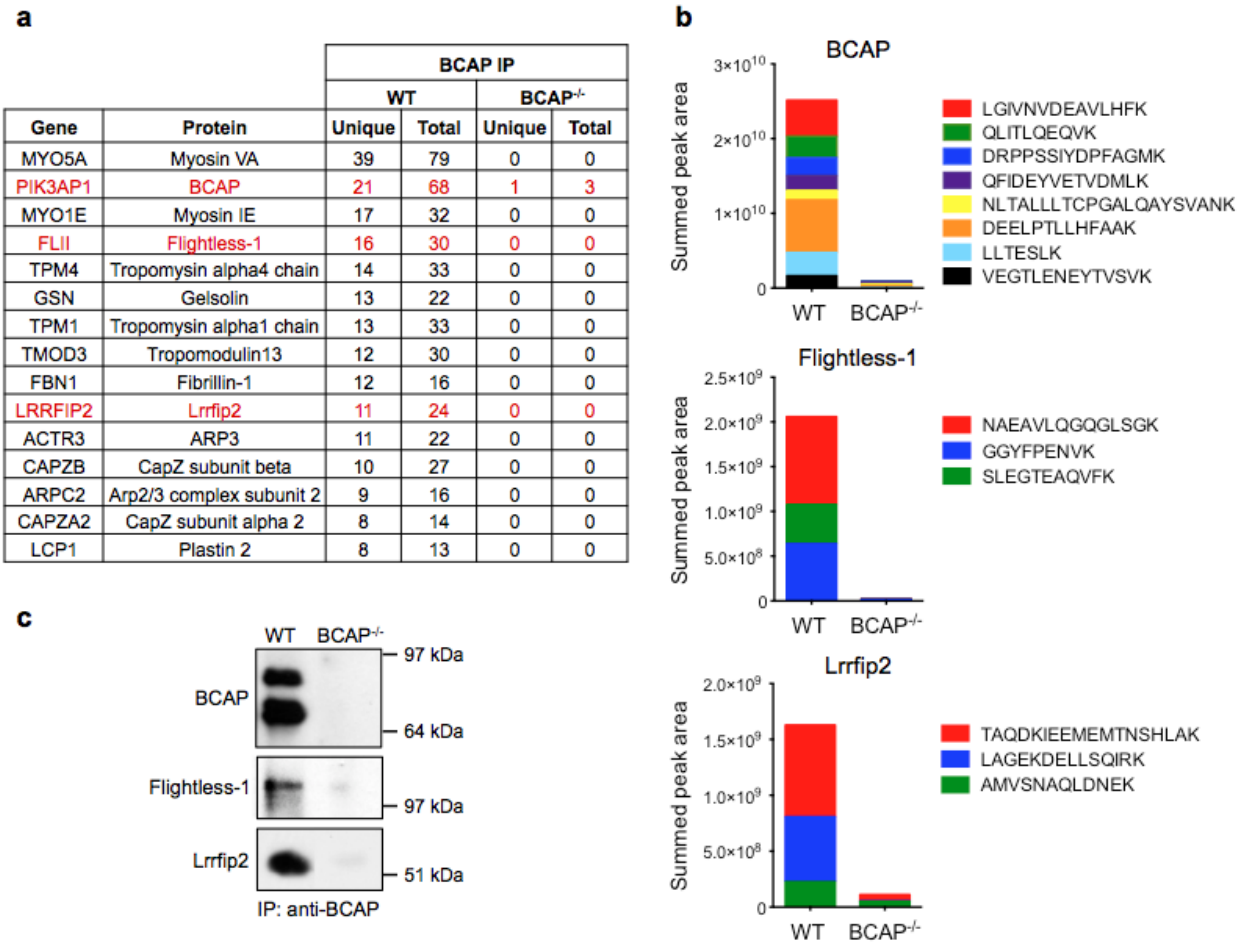

Figure 2.4. BCAP interacts with Flightless-1 in macrophages. (a) Compiled mass spectrometry results from anti-BCAP immunoprecipitations (IPs) from WT (n=3) or BCAP$^{-/-}$ (n=1) BMDM. The average numbers of unique and total peptides from each protein are shown from proteins with ≥5 unique peptides in anti-BCAP IPs from WT BMDM and ≤2 peptides in the control IP from BCAP$^{-/-}$ BMDM. Proteins with a high likelihood of non-specific binding as determined by >10 average spectral counts in the CRAPome database were also excluded. BCAP (encoded by *Pik3ap1*), Flightless-1 (encoded by *Flii*), and Lrrfip2 (encoded by *Lrrfip2*) are highlighted in red. (b) Label free quantitative proteomics data are shown for the indicated high intensity peptides found from the indicated proteins in WT and BCAP$^{-/-}$ immunoprecipitates. The colored bars represent the mean peak area quantification of the precursor ions for each peptide from a representative experiment. The intensity of each peptide was summed to generate an overall protein quantification score (peak area). (c) Cytoplasmic extracts from WT or BCAP$^{-/-}$ macrophages were immunoprecipitated with anti-BCAP mAb, separated by SDS-PAGE, and Western blotted for BCAP, Flightless-1 (Flii) or Lrrfip2. Data are representative of at least three independent experiments.

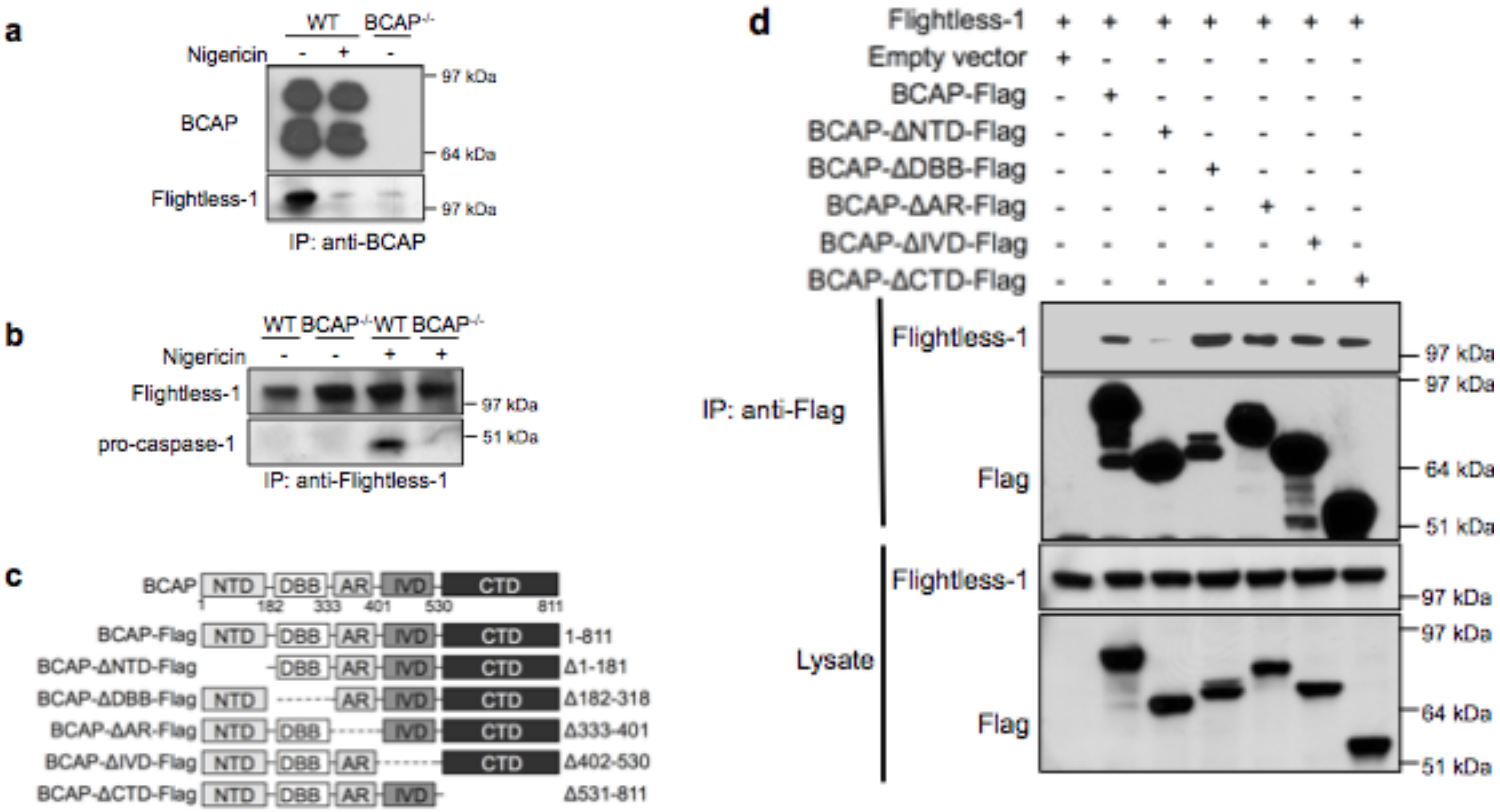

Figure 2.5. Flightless-1 interaction with caspase-1 during NLRP3 inflammasome activation requires BCAP. (a) WT or BCAP$^{-/-}$ macrophages were primed with 10 ng/ml LPS for 4 hours, treated with or without 5 μM nigericin for 15 minutes, then lysed and immunoprecipitated with anti-BCAP monoclonal antibody, separated by SDS-PAGE and Western blotted for Flightless-1 or BCAP. (b) Macrophages treated as in (a) were lysed and immunoprecipitated with anti-Flightless-1 monoclonal antibody, separated by SDS-page and immunoblotted for Flightless-1 or caspase-1. (c) Schematic of BCAP protein domains and Flag-tagged BCAP mutants used in (d). NTD, N-terminal domain; DBB, Dof-BCAP-BANK1 domain; AR, Ankyrin repeats; IVD, intervening domain; CTD, C-terminal domain. Numbers on right denote deleted amino acids. (d) Flag-tagged BCAP mutants and Flightless-1 were cotransfected into 293T cells, then lysed and immunoprecipitated with anti-Flag monoclonal antibody. Lysates and immunoprecipitates were separated by SDS-PAGE and immunoblotted for Flag or Flightless-1. Data are representative of three independent experiments (a,b,d).

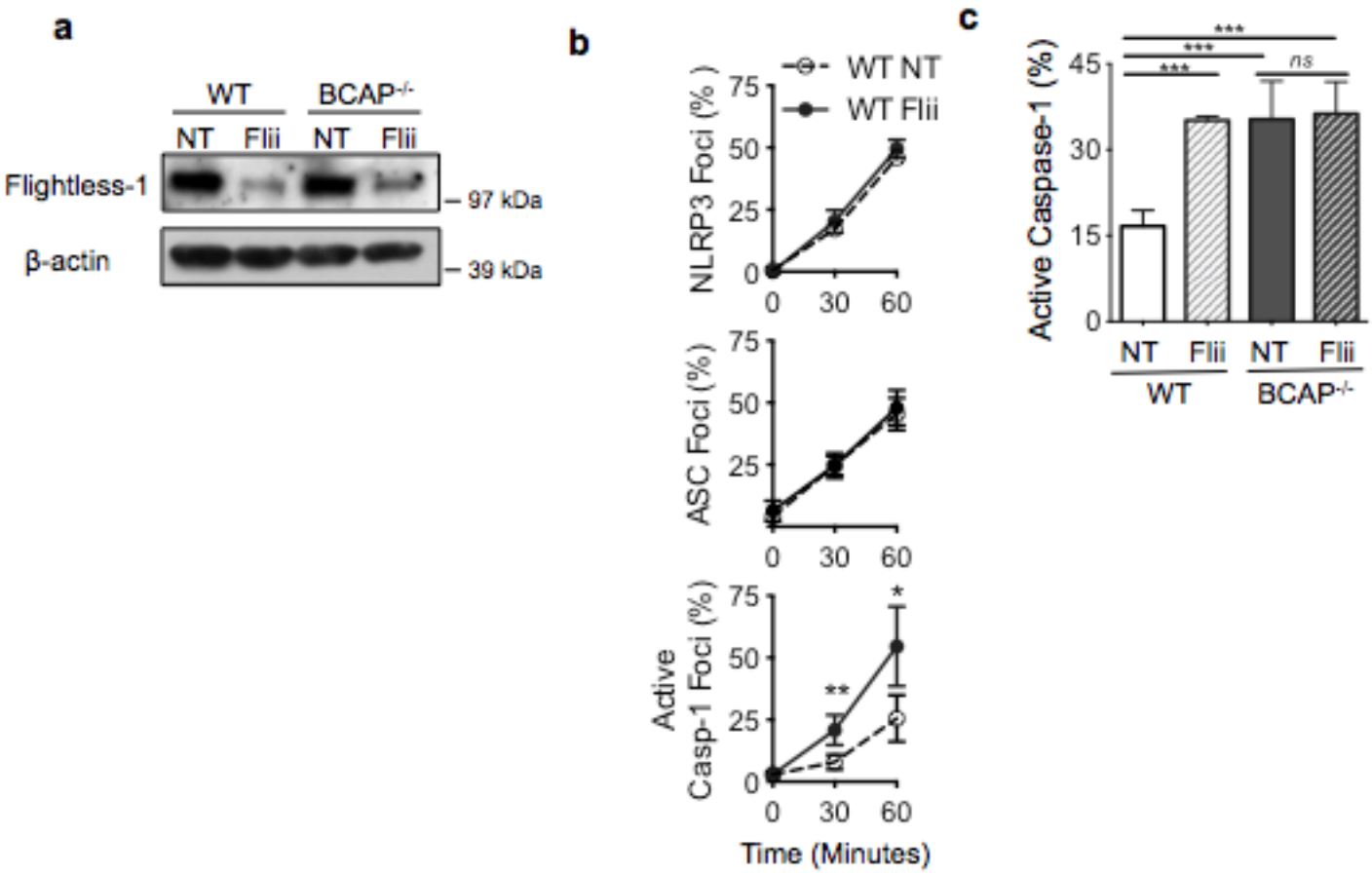

Figure 2.6. BCAP inhibition of inflammasome activation requires Flightless-1. (a) Western blot of Flightless-1 knockdown in WT and BCAP$^{-/-}$ macrophages. BMDM were infected with lentiviruses encoding non-targeting (NT) or Flightless-1 (Flii)-specific shRNA and selected with puromycin. Cytoplasmic extracts were Western blotted for Flightless-1 or β-actin. (b) LPS-primed WT BMDM infected with NT or Flii-specific shRNA were infected with *YpstbΔ* and NLRP3, ASC, and active caspase-1 were stained and quantified by immunofluorescence as in Fig. 3. (c) WT and BCAP$^{-/-}$ BMDM were infected with *YpstbΔ* for 60 min and stained for active caspase-1 with FAM-YVAD-FMK. Percent of cells with active caspase-1 was quantified by immunofluorescence. *ns*, not significant, **p*<.05, ***p* <.01, ****p*<.001 (b, Student's *t*-test) (c, One way ANOVA with Tukey's post-test). Data are representative of three (a,b,c) independent experiments. Data presented are mean +/- SD (b) or + SD.

Chapter 5. Future Directions

YopM Future Directions

Our data show $YopM_{399}$ inhibits caspase-1 enzymatic function comparably to full-length YopM, yet we observed $YopM_{399}$ has an intermediate phenotype of caspase-1 inhibition, cell lysis, and IL-1β release during *Yersinia* infections involving intact macrophages. These data argue cellular context is important for the contributions of the C-terminus of YopM during infection, which we demonstrate is due to the ability of YopM to block recruitment of caspase-1 to pre-inflammasome foci. Because the C-terminus of YopM is also required for YopM interactions with Rsk1, it is possible Rsk1 acts as an anchoring protein that obstructs recruitment of the YopM/pro-caspase-1 complex to pre-inflammasome foci. Appropriate spatial and temporal distribution is important for kinase signaling (78); therefore it is possible that Rsk1 spatial distribution is regulated by the host to facilitate optimal kinase activity. *Yersinia* may take advantage of Rsk1 spatial distribution through protein-protein interactions that inhibit recruitment of pro-caspase-1 to the inflammasome. YopM also stimulates the kinase activity of Rsk1 (55, 56), which may contribute to *Yersinia* pathogenesis independent of inflammasome inhibition. However, restoration of virulence to *Yersinia* deficient in the ability to increase Rsk1 kinase activity (*$yopM_{399}$*) in *caspase-1/-11* knockout mice argues that this may be a minor mechanism during pathogenesis. In addition to Rsk1, other YopM-interacting partners may also play a role in spatial regulation of YopM. Alternatively, the C-terminus of YopM may interfere with interactions between CARD domains of pro-caspase-1 and ASC, blocking recruitment of pro-caspase-1 to pre-inflammasomes. Future work will be needed to investigate the interplay between YopM, YopM interacting partners, and pro-caspase-1.

BCAP Future Directions

An outstanding question is whether BCAP and Flightless-1 inhibit the non-canonical caspase-11 inflammasome that senses cytosolic LPS. Flightless-1 was first identified as a caspase-11 interacting protein and was subsequently found to bind to caspase-1(41). Interestingly, Flightless-1 does not inhibit the enzymatic activity of caspase-11 in vitro, only that of caspase-1(41). If Flightless-1 and BCAP inhibit the caspase-11 inflammasome in macrophages, it would suggest that the ability of Flightless-1 to act as an enzymatic pseudosubstrate inhibitor is not required for inhibition of non-canonical inflammasome formation, and that it is the ability of Flightless-1 to delay entry of pro-caspase-11 into the forming inflammasome that is critical for its function. Future work will assess the spectrum of inflammasomes that are inhibited by BCAP and Flightless-1.

We and others have shown that activation of the NLRP3 inflammasome induces the association of pro-caspase-1 and Flightless-1 in macrophages (72). We propose that BCAP acts as a scaffold that aids in recruitment of pro-caspase-1 to Flightless-1, as we observed Flightless-1 and pro-caspase-1 do not associate in BCAP$^{-/-}$ macrophages and therefore Flightless-1 cannot function in the absence of BCAP. BCAP releases the Flightless-1-pro-caspase-1 complex once formed. Because the interaction between BCAP and Flightless-1 is lost after nigericin treatment, it is possible that this dissociation is driven by NLRP3-initiated post-translational modifications of these proteins. Interestingly, the opposite is true for the interaction between Flightless-1 and pro-caspase-1, as Flightless-1 and pro-caspase-1 only associate in WT macrophages after treatment with nigericin. This suggests an intracellular signal leads to Flightless-1 recruitment of pro-caspase-1, perhaps the same signal that leads to release of BCAP. Post translational modifications such as phosphorylation, ubiquitylation, and S-nitrosylation have all been

implicated in regulating inflammasome assembly and activation(79), suggesting post-translational modifications could be responsible for controlling interactions between Flightless-1 and BCAP and/or Flightless-1 and pro-caspase-1. BCAP also interacts with the Flightless-1 binding protein Lrrfip2(80). Lrrfip2 participates in Flightless-1 inhibition of the NLRP3 inflammasome. But, unlike BCAP, Lrrfip2 does not contribute to inhibition of the NLRC4 inflammasome(72), suggesting BCAP and Lrrfip2 play distinct roles in inhibition of inflammasome activation. Future work could investigate the interplay between BCAP, Lrrfip2 and Flightless-1 in inhibition of inflammasomes initiated by distinct sensors.

In summary, both host and pathogen employ similar mechanisms to limit inflammatory responses. Pathogens evade inflammasome activation to efficiently colonize the host, while the host limits inflammation to prevent excess collateral damage associated with inflammasome activation. These studies demonstrate spatial regulation of caspase-1 recruitment to inflammasomes is an important mechanism of dampening the host immune defense.

Bibliography

1. **Stenseth NC, Atshabar BB, Begon M, Belmain SR, Bertherat E, Carniel E, Gage KL, Leirs H, Rahalison L.** 2008. Plague: past, present, and future. PLoS Med **5:**e3.
2. **Galimand M, Guiyoule A, Gerbaud G, Rasoamanana B, Chanteau S, Carniel E, Courvalin P.** 1997. Multidrug resistance in Yersinia pestis mediated by a transferable plasmid. N Engl J Med **337:**677-680.
3. **Price PA, Jin J, Goldman WE.** 2012. Pulmonary infection by Yersinia pestis rapidly establishes a permissive environment for microbial proliferation. Proc Natl Acad Sci U S A **109:**3083-3088.
4. **Lathem WW, Price PA, Miller VL, Goldman WE.** 2007. A plasminogen-activating protease specifically controls the development of primary pneumonic plague. Science **315:**509-513.
5. **Bergsbaken T, Cookson BT.** 2007. Macrophage activation redirects yersinia-infected host cell death from apoptosis to caspase-1-dependent pyroptosis. PLoS Pathog **3:**e161.
6. **Peters KN, Dhariwala MO, Hughes Hanks JM, Brown CR, Anderson DM.** 2013. Early apoptosis of macrophages modulated by injection of Yersinia pestis YopK promotes progression of primary pneumonic plague. PLoS Pathog **9:**e1003324.
7. **Achtman M, Zurth K, Morelli G, Torrea G, Guiyoule A, Carniel E.** 1999. Yersinia pestis, the cause of plague, is a recently emerged clone of Yersinia pseudotuberculosis. Proc Natl Acad Sci U S A **96:**14043-14048.
8. **Ben-Gurion R, Shafferman A.** 1981. Essential virulence determinants of different Yersinia species are carried on a common plasmid. Plasmid **5:**183-187.

9. **Bliska JB, Wang X, Viboud GI, Brodsky IE.** 2013. Modulation of innate immune responses by Yersinia type III secretion system translocators and effectors. Cell Microbiol **15:**1622-1631.

10. **LaRock CN, Cookson BT.** 2012. The Yersinia Virulence Effector YopM Binds Caspase-1 to Arrest Inflammasome Assembly and Processing. Cell Host Microbe **12:**799-805.

11. **von Moltke J, Ayres JS, Kofoed EM, Chavarría-Smith J, Vance RE.** 2013. Recognition of bacteria by inflammasomes. Annu Rev Immunol **31:**73-106.

12. **LaRock CN, Cookson BT.** 2013. Burning down the house: cellular actions during pyroptosis. PLoS Pathog **9:**e1003793.

13. **Rock KL, Latz E, Ontiveros F, Kono H.** 2010. The sterile inflammatory response. Annu Rev Immunol **28:**321-342.

14. **Broderick L, De Nardo D, Franklin BS, Hoffman HM, Latz E.** 2015. The inflammasomes and autoinflammatory syndromes. Annu Rev Pathol **10:**395-424.

15. **Cai X, Chen J, Xu H, Liu S, Jiang QX, Halfmann R, Chen ZJ.** 2014. Prion-like polymerization underlies signal transduction in antiviral immune defense and inflammasome activation. Cell **156:**1207-1222.

16. **Lu A, Magupalli VG, Ruan J, Yin Q, Atianand MK, Vos MR, Schröder GF, Fitzgerald KA, Wu H, Egelman EH.** 2014. Unified polymerization mechanism for the assembly of ASC-dependent inflammasomes. Cell **156:**1193-1206.

17. **Hauenstein AV, Zhang L, Wu H.** 2015. The hierarchical structural architecture of inflammasomes, supramolecular inflammatory machines. Curr Opin Struct Biol **31:**75-83.

18. **Broz P, von Moltke J, Jones JW, Vance RE, Monack DM.** 2010. Differential requirement for Caspase-1 autoproteolysis in pathogen-induced cell death and cytokine processing. Cell Host Microbe **8:**471-483.

19. **Shi J, Zhao Y, Wang K, Shi X, Wang Y, Huang H, Zhuang Y, Cai T, Wang F, Shao F.** 2015. Cleavage of GSDMD by inflammatory caspases determines pyroptotic cell death. Nature **526:**660-665.

20. **Kayagaki N, Stowe IB, Lee BL, O'Rourke K, Anderson K, Warming S, Cuellar T, Haley B, Roose-Girma M, Phung QT, Liu PS, Lill JR, Li H, Wu J, Kummerfeld S, Zhang J, Lee WP, Snipas SJ, Salvesen GS, Morris LX, Fitzgerald L, Zhang Y, Bertram EM, Goodnow CC, Dixit VM.** 2015. Caspase-11 cleaves gasdermin D for non-canonical inflammasome signalling. Nature **526:**666-671.

21. **Stewart MK, Cookson BT.** 2016. Evasion and interference: intracellular pathogens modulate caspase-dependent inflammatory responses. Nat Rev Microbiol **14:**346-359.

22. **Franklin BS, Bossaller L, De Nardo D, Ratter JM, Stutz A, Engels G, Brenker C, Nordhoff M, Mirandola SR, Al-Amoudi A, Mangan MS, Zimmer S, Monks BG, Fricke M, Schmidt RE, Espevik T, Jones B, Jarnicki AG, Hansbro PM, Busto P, Marshak-Rothstein A, Hornemann S, Aguzzi A, Kastenmüller W, Latz E.** 2014. The adaptor ASC has extracellular and 'prionoid' activities that propagate inflammation. Nat Immunol **15:**727-737.

23. **Bergsbaken T, Fink SL, Cookson BT.** 2009. Pyroptosis: host cell death and inflammation. Nat Rev Microbiol **7:**99-109.

24. **Lupfer C, Kanneganti TD.** 2013. The expanding role of NLRs in antiviral immunity. Immunol Rev **255:**13-24.

25. **Yen H, Sugimoto N, Tobe T.** 2015. Enteropathogenic Escherichia coli Uses NleA to Inhibit NLRP3 Inflammasome Activation. PLoS Pathog **11:**e1005121.

26. **Dorfleutner A, Talbott SJ, Bryan NB, Funya KN, Rellick SL, Reed JC, Shi X, Rojanasakul Y, Flynn DC, Stehlik C.** 2007. A Shope Fibroma virus PYRIN-only protein modulates the host immune response. Virus Genes **35:**685-694.

27. **Johnston JB, Barrett JW, Nazarian SH, Goodwin M, Ricciuto D, Ricuttio D, Wang G, McFadden G.** 2005. A poxvirus-encoded pyrin domain protein interacts with ASC-1 to inhibit host inflammatory and apoptotic responses to infection. Immunity **23:**587-598.

28. **Lemaître N, Sebbane F, Long D, Hinnebusch BJ.** 2006. Yersinia pestis YopJ suppresses tumor necrosis factor alpha induction and contributes to apoptosis of immune cells in the lymph node but is not required for virulence in a rat model of bubonic plague. Infect Immun **74:**5126-5131.

29. **Orth K, Palmer LE, Bao ZQ, Stewart S, Rudolph AE, Bliska JB, Dixon JE.** 1999. Inhibition of the mitogen-activated protein kinase kinase superfamily by a Yersinia effector. Science **285:**1920-1923.

30. **Orth K, Xu Z, Mudgett MB, Bao ZQ, Palmer LE, Bliska JB, Mangel WF, Staskawicz B, Dixon JE.** 2000. Disruption of signaling by Yersinia effector YopJ, a ubiquitin-like protein protease. Science **290:**1594-1597.

31. **Zhou H, Monack DM, Kayagaki N, Wertz I, Yin J, Wolf B, Dixit VM.** 2005. Yersinia virulence factor YopJ acts as a deubiquitinase to inhibit NF-kappa B activation. J Exp Med **202:**1327-1332.

32. **Navarro L, Alto NM, Dixon JE.** 2005. Functions of the Yersinia effector proteins in inhibiting host immune responses. Curr Opin Microbiol **8:**21-27.

33. **Brodsky IE, Palm NW, Sadanand S, Ryndak MB, Sutterwala FS, Flavell RA, Bliska JB, Medzhitov R.** 2010. A Yersinia effector protein promotes virulence by preventing inflammasome recognition of the type III secretion system. Cell Host Microbe **7:**376-387.

34. **Lamkanfi M, Dixit VM.** 2009. The inflammasomes. PLoS Pathog **5:**e1000510.

35. **Silverman GA, Bird PI, Carrell RW, Church FC, Coughlin PB, Gettins PG, Irving JA, Lomas DA, Luke CJ, Moyer RW, Pemberton PA, Remold-O'Donnell E, Salvesen GS, Travis J, Whisstock JC.** 2001. The serpins are an expanding superfamily of structurally similar but functionally diverse proteins. Evolution, mechanism of inhibition, novel functions, and a revised nomenclature. J Biol Chem **276:**33293-33296.

36. **Le HT, Harton JA.** 2013. Pyrin- and CARD-only Proteins as Regulators of NLR Functions. Front Immunol **4:**275.

37. **Dorfleutner A, Chu L, Stehlik C.** 2015. Inhibiting the inflammasome: one domain at a time. Immunol Rev **265:**205-216.

38. **Chen S, Sun B.** 2013. Negative regulation of NLRP3 inflammasome signaling. Protein Cell **4:**251-258.

39. **Young JL, Sukhova GK, Foster D, Kisiel W, Libby P, Schönbeck U.** 2000. The serpin proteinase inhibitor 9 is an endogenous inhibitor of interleukin 1beta-converting enzyme (caspase-1) activity in human vascular smooth muscle cells. J Exp Med **191:**1535-1544.

40. **Annand RR, Dahlen JR, Sprecher CA, De Dreu P, Foster DC, Mankovich JA, Talanian RV, Kisiel W, Giegel DA.** 1999. Caspase-1 (interleukin-1beta-converting enzyme) is inhibited by the human serpin analogue proteinase inhibitor 9. Biochem J **342 Pt 3:**655-665.

41. **Li J, Yin HL, Yuan J.** 2008. Flightless-I regulates proinflammatory caspases by selectively modulating intracellular localization and caspase activity. J Cell Biol **181:**321-333.

42. **Fink SL, Cookson BT.** 2006. Caspase-1-dependent pore formation during pyroptosis leads to osmotic lysis of infected host macrophages. Cell Microbiol **8:**1812-1825.

43. **Yamazaki T, Takeda K, Gotoh K, Takeshima H, Akira S, Kurosaki T.** 2002. Essential immunoregulatory role for BCAP in B cell development and function. J Exp Med **195:**535-545.

44. **MacFarlane AW, Yamazaki T, Fang M, Sigal LJ, Kurosaki T, Campbell KS.** 2008. Enhanced NK-cell development and function in BCAP-deficient mice. Blood **112:**131-140.

45. **Eng JK, Jahan TA, Hoopmann MR.** 2013. Comet: an open-source MS/MS sequence database search tool. Proteomics **13:**22-24.

46. **Keller A, Eng J, Zhang N, Li XJ, Aebersold R.** 2005. A uniform proteomics MS/MS analysis platform utilizing open XML file formats. Molecular systems biology **1:**2005 0017.

47. **MacLean B, Tomazela DM, Shulman N, Chambers M, Finney GL, Frewen B, Kern R, Tabb DL, Liebler DC, MacCoss MJ.** 2010. Skyline: an open source document editor for creating and analyzing targeted proteomics experiments. Bioinformatics **26:**966-968.

48. **Viboud GI, So SS, Ryndak MB, Bliska JB.** 2003. Proinflammatory signalling stimulated by the type III translocation factor YopB is counteracted by multiple effectors in epithelial cells infected with Yersinia pseudotuberculosis. Mol Microbiol **47:**1305-1315.

49. **von Moltke J, Trinidad NJ, Moayeri M, Kintzer AF, Wang SB, van Rooijen N, Brown CR, Krantz BA, Leppla SH, Gronert K, Vance RE.** 2012. Rapid induction of inflammatory lipid mediators by the inflammasome in vivo. Nature **490:**107-111.

50. **Yamazaki T, Kurosaki T.** 2003. Contribution of BCAP to maintenance of mature B cells through c-Rel. Nat Immunol **4:**780-786.

51. **Evdokimov AG, Anderson DE, Routzahn KM, Waugh DS.** 2001. Unusual molecular architecture of the Yersinia pestis cytotoxin YopM: a leucine-rich repeat protein with the shortest repeating unit. J Mol Biol **312:**807-821.

52. **Kloss E, Barrick D.** 2009. C-terminal deletion of leucine-rich repeats from YopM reveals a heterogeneous distribution of stability in a cooperatively folded protein. Protein Sci **18:**1948-1960.

53. **McPhee JB, Mena P, Bliska JB.** 2010. Delineation of regions of the Yersinia YopM protein required for interaction with the RSK1 and PRK2 host kinases and their requirement for interleukin-10 production and virulence. Infect Immun **78:**3529-3539.

54. **McCoy MW, Marré ML, Lesser CF, Mecsas J.** 2010. The C-terminal tail of Yersinia pseudotuberculosis YopM is critical for interacting with RSK1 and for virulence. Infect Immun **78:**2584-2598.

55. **Hentschke M, Berneking L, Belmar Campos C, Buck F, Ruckdeschel K, Aepfelbacher M.** 2010. Yersinia virulence factor YopM induces sustained RSK activation by interfering with dephosphorylation. PLoS One **5**.

56. **McDonald C, Vacratsis PO, Bliska JB, Dixon JE.** 2003. The yersinia virulence factor YopM forms a novel protein complex with two cellular kinases. J Biol Chem **278:**18514-18523.

57. **Sapkota GP, Cummings L, Newell FS, Armstrong C, Bain J, Frodin M, Grauert M, Hoffmann M, Schnapp G, Steegmaier M, Cohen P, Alessi DR.** 2007. BI-D1870 is a specific inhibitor of the p90 RSK (ribosomal S6 kinase) isoforms in vitro and in vivo. Biochem J **401:**29-38.

58. **Lathem WW, Crosby SD, Miller VL, Goldman WE.** 2005. Progression of primary pneumonic plague: a mouse model of infection, pathology, and bacterial transcriptional activity. Proc Natl Acad Sci U S A **102:**17786-17791.

59. **Wu H.** 2013. Higher-order assemblies in a new paradigm of signal transduction. Cell **153:**287-292.

60. **Kagan JC, Magupalli VG, Wu H.** 2014. SMOCs: supramolecular organizing centres that control innate immunity. Nat Rev Immunol **14:**821-826.

61. **Guo H, Callaway JB, Ting JP.** 2015. Inflammasomes: mechanism of action, role in disease, and therapeutics. Nat Med **21:**677-687.

62. **Doherty TA, Brydges SD, Hoffman HM.** 2011. Autoinflammation: translating mechanism to therapy. J Leukoc Biol **90:**37-47.

63. **Brydges SD, Broderick L, McGeough MD, Pena CA, Mueller JL, Hoffman HM.** 2013. Divergence of IL-1, IL-18, and cell death in NLRP3 inflammasomopathies. J Clin Invest **123:**4695-4705.

64. **Thornberry NA, Bull HG, Calaycay JR, Chapman KT, Howard AD, Kostura MJ, Miller DK, Molineaux SM, Weidner JR, Aunins J.** 1992. A novel heterodimeric cysteine protease is required for interleukin-1 beta processing in monocytes. Nature **356:**768-774.

65. **Okada T, Maeda A, Iwamatsu A, Gotoh K, Kurosaki T.** 2000. BCAP: the tyrosine kinase substrate that connects B cell receptor to phosphoinositide 3-kinase activation. Immunity **13:**817-827.

66. **Ni M, MacFarlane AW, Toft M, Lowell CA, Campbell KS, Hamerman JA.** 2012. B-cell adaptor for PI3K (BCAP) negatively regulates Toll-like receptor signaling through activation of PI3K. Proc Natl Acad Sci U S A **109:**267-272.

67. **Troutman TD, Hu W, Fulenchek S, Yamazaki T, Kurosaki T, Bazan JF, Pasare C.** 2012. Role for B-cell adapter for PI3K (BCAP) as a signaling adapter linking Toll-like receptors (TLRs) to serine/threonine kinases PI3K/Akt. Proc Natl Acad Sci U S A **109:**273-278.

68. **Battersby A, Csiszár A, Leptin M, Wilson R.** 2003. Isolation of proteins that interact with the signal transduction molecule Dof and identification of a functional domain conserved between Dof and vertebrate BCAP. J Mol Biol **329:**479-493.

69. **Miao EA, Rajan JV.** 2011. Salmonella and Caspase-1: A complex Interplay of Detection and Evasion. Front Microbiol **2:**85.

70. **Fink SL, Bergsbaken T, Cookson BT.** 2008. Anthrax lethal toxin and Salmonella elicit the common cell death pathway of caspase-1-dependent pyroptosis via distinct mechanisms. Proc Natl Acad Sci U S A **105:**4312-4317.

71. **Mellacheruvu D, Wright Z, Couzens AL, Lambert JP, St-Denis NA, Li T, Miteva YV, Hauri S, Sardiu ME, Low TY, Halim VA, Bagshaw RD, Hubner NC, Al-Hakim A, Bouchard A, Faubert D, Fermin D, Dunham WH, Goudreault M, Lin ZY, Badillo BG, Pawson T, Durocher D, Coulombe B, Aebersold R, Superti-Furga G, Colinge J, Heck AJ, Choi H, Gstaiger M, Mohammed S, Cristea IM, Bennett KL,**

Washburn MP, Raught B, Ewing RM, Gingras AC, Nesvizhskii AI. 2013. The CRAPome: a contaminant repository for affinity purification-mass spectrometry data. Nat Methods **10:**730-736.

72. **Jin J, Yu Q, Han C, Hu X, Xu S, Wang Q, Wang J, Li N, Cao X.** 2013. LRRFIP2 negatively regulates NLRP3 inflammasome activation in macrophages by promoting Flightless-I-mediated caspase-1 inhibition. Nat Commun **4:**2075.

73. **Huang dW, Sherman BT, Lempicki RA.** 2009. Systematic and integrative analysis of large gene lists using DAVID bioinformatics resources. Nat Protoc **4:**44-57.

74. **Huang dW, Sherman BT, Lempicki RA.** 2009. Bioinformatics enrichment tools: paths toward the comprehensive functional analysis of large gene lists. Nucleic Acids Res **37:**1-13.

75. **Man SM, Ekpenyong A, Tourlomousis P, Achouri S, Cammarota E, Hughes K, Rizzo A, Ng G, Wright JA, Cicuta P, Guck JR, Bryant CE.** 2014. Actin polymerization as a key innate immune effector mechanism to control Salmonella infection. Proc Natl Acad Sci U S A **111:**17588-17593.

76. **Xu H, Yang J, Gao W, Li L, Li P, Zhang L, Gong YN, Peng X, Xi JJ, Chen S, Wang F, Shao F.** 2014. Innate immune sensing of bacterial modifications of Rho GTPases by the Pyrin inflammasome. Nature **513:**237-241.

77. **Kim ML, Chae JJ, Park YH, De Nardo D, Stirzaker RA, Ko HJ, Tye H, Cengia L, DiRago L, Metcalf D, Roberts AW, Kastner DL, Lew AM, Lyras D, Kile BT, Croker BA, Masters SL.** 2015. Aberrant actin depolymerization triggers the pyrin inflammasome and autoinflammatory disease that is dependent on IL-18, not IL-1β. J Exp Med **212:**927-938.

78. **Edwards AS, Scott JD.** 2000. A-kinase anchoring proteins: protein kinase A and beyond. Curr Opin Cell Biol **12:**217-221.

79. **Man SM, Kanneganti TD.** 2015. Regulation of inflammasome activation. Immunol Rev **265:**6-21.

80. **Dai P, Jeong SY, Yu Y, Leng T, Wu W, Xie L, Chen X.** 2009. Modulation of TLR signaling by multiple MyD88-interacting partners including leucine-rich repeat Fli-I-interacting proteins. J Immunol **182:**3450-3460.

Samuel Carpentier

UW Microbiology
Campus Box 357735
Seattle, WA 98195

sjcarpen@uw.edu
206.543.9025 (work)
843.532.9661 (personal)

Education

Ph.D Dept. of Microbiology, University of Washington, Seattle, WA 2016

B.S Microbiology, University of Michigan, Ann Arbor, MI 2011

Research Experience

Graduate Studies 2011-2016
University of Washington Dept. of Microbiology, Seattle, Washington
Advisor **Brad T. Cookson M.D, Ph.D.**
Investigating negative regulation of inflammasome activation

Undergraduate Researcher 2009-2011
University of Michigan Dept. of Microbiology & Immunology, Ann Arbor, Michigan
Advisor **Victor DiRita, Ph.D.**
Investigating a bottleneck of co-colonization of Campylobacter jejuni in the chicken

Undergraduate Researcher 2009
University of Oregon Institute of Molecular Biology, Eugene, Oregon
Advisor **Karen Guillemin, Ph.D.**
Characterizing intestinal inflammation in Fanconi Anemia zebrafish mutants

Undergraduate Researcher 2008
Medical University of South Carolina Dept. of Neuroscience, Charleston, South Carolina
Advisor **James Cook, PhD.**
Identifying the effects of ß-arrestin 2 on inflammatory responses in murine bone marrow-derived macrophages

Academic Honors and Awards

Poster Award, University of Washington Department of Microbiology Retreat 2015

Fellowship, University of Washington Cell and Molecular Biology Training Grant 2012-15

Poster Award, Annual Biomedical Research Conference for Minority Students 2009

Travel Award, Federation of American Societies for Experimental Biology Minority Access to Research Careers (MARC) 2009

Outstanding Summer Research Award, Medical University of South Carolina 2008

Scholarship, Michigan Out of State Scholar 2007-2011

Professional Organizations & Service

STEM OUT Mentor 2014-16
TAF Academy, Seattle, WA

PAWS-On Science, Microbiology Volunteer, 2014, 2015
Pacific Science Center, Kent, WA

Student President, 2014-2015
University of Washington Dept. of Microbiology

Student Faculty Representative, 2013-2014
University of Washington Dept. of Microbiology

Graduate Recruitment Organizer, 2012-2013
University of Washington Dept. of Microbiology

Seattle Science Festival, Microbiology Volunteer 2012, 2013
Pacific Science Center, Seattle, WA

Publications

Johnson JG, **Carpentier S**, Spurbeck RR, Sandhu SK, DiRita VJ. 2014. Genome sequences of Campylobacter jejuni 81-176 variants with enhanced fitness relative to the parental strain in the chicken gastrointestinal tract. **Genome Announc**. 2(1):e00006-14. doi:10.1128/genomeA.00006-14.

Teaching Experience

Guest Lecturer, *Staphylococci*, Medical Bacteriology (Micro 442), 2015
Univ. of Washington

Guest Lecturer, *Polymerase Chain Reaction*, Prokaryotic Recombinant 2015
DNA Techniques (Micro 431), Univ. of Washington

Teaching Assistant, Fundamentals of General Microbiology (Micro 402) 2012

Teaching Assistant, Bacterial Genetics (Micro 411) 2013

Presentations

Seattle Area Microbial Pathogenesis Work-in-Progress Meeting 2015
University of Washington, Seattle, WA

Seattle Area Microbial Pathogenesis Work-in-Progress Meeting 2014
University of Washington, Seattle, WA

University of Washington Department of Microbiology Retreat 2013
Talaris Conference Center, Seattle, WA

University of Michigan Department of Microbiology and Immunology 2010
Undergraduate Summer Research Presentation
University of Michigan, Ann Arbor, MI

Poster, **Annual Biomedical Research Conference for Minority Students** 2009

Phoenix Convention Center, Phoenix, AZ

University of Oregon Summer Program for Undergraduate Research 2009
University of Oregon, Eugene, OR

Medical University of South Carolina Summer Research Program 2008
Medical University of South Carolina, Charleston, SC